Provided for non-commercial research and education use.
Not for reproduction, distribution or commercial use.

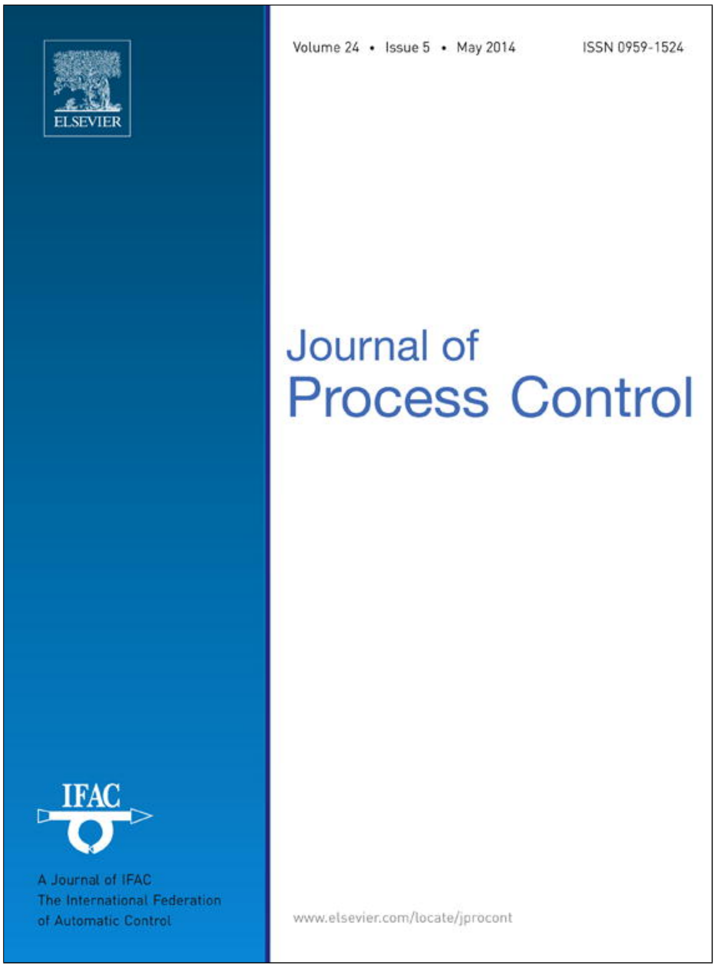

This article appeared in a journal published by Elsevier. The attached copy is furnished to the author for internal non-commercial research and education use, including for instruction at the authors institution and sharing with colleagues.

Other uses, including reproduction and distribution, or selling or licensing copies, or posting to personal, institutional or third party websites are prohibited.

In most cases authors are permitted to post their version of the article (e.g. in Word or Tex form) to their personal website or institutional repository. Authors requiring further information regarding Elsevier's archiving and manuscript policies are encouraged to visit:

http://www.elsevier.com/authorsrights

Author's personal copy

Journal of Process Control 24 (2014) 550–567

Contents lists available at ScienceDirect

Journal of Process Control

journal homepage: www.elsevier.com/locate/jprocont

L_2 disturbance attenuation for highly dissipative nonlinear spatially distributed processes via HJI approach

Huai-Ning Wu*, Biao Luo

Science and Technology on Aircraft Control Laboratory, School of Automation Science and Electrical Engineering, Beihang University (Beijing University of Aeronautics and Astronautics), Beijing 100191, PR China

ARTICLE INFO

Article history:
Received 9 January 2013
Received in revised form 1 September 2013
Accepted 23 February 2014
Available online 1 May 2014

Keywords:
Process control
Transport processes
Model reduction
Chemical reactors
Spatially distributed process
Hamilton–Jacobi–Isaacs equation

ABSTRACT

For many practical industrial spatially distributed processes (SDPs), their dynamics are usually described by highly dissipative nonlinear partial differential equations (PDEs). In this paper, we address the L_2 disturbance attenuation problem of nonlinear SDPs using the Hamilton–Jacobi–Isaacs (HJI) approach. Firstly, by collecting an ensemble of PDE states, Karhunen–Loève decomposition (KLD) is employed to compute empirical eigenfunctions (EEFs) of the SDP based on the method of snapshots. Subsequently, these EEFs together with singular perturbation (SP) technique are used to obtain a finite-dimensional slow subsystem of ordinary differential equation (ODE) that accurately describes the dominant dynamics of the PDE system. Secondly, based on the slow subsystem, the L_2 disturbance attenuation problem is reformulated and a finite-dimensional H_∞ controller is synthesized in terms of the HJI equation. Moreover, the stability and L_2-gain performance of the closed-loop PDE system are analyzed. Thirdly, since the HJI equation is a nonlinear PDE that has proven to be impossible to solve analytically, we combine the method of weighted residuals (MWR) and simultaneous policy update algorithm (SPUA) to obtain its approximate solution. Finally, the simulation studies are conducted on a nonlinear diffusion-reaction process and a temperature cooling fin of high-speed aerospace vehicle, and the achieved results demonstrate the effectiveness of the developed control method.

© 2014 Elsevier Ltd. All rights reserved.

1. Introduction

It is ubiquitous that many industrial processes exhibit significant spatial variations owing to the underlying physical phenomena, such as diffusion, convection, phase-dispersion, vibration, flow, etc. Typical examples include the catalytic packed-bed reactors [1,2] used to convert methanol to formaldehyde, the Czochralski crystallization [3] of high-purity crystals, the chemical vapor deposition [4,5] of thin films for microelectronics manufacturing, the aerosol-based production of nanoparticles [6] used in medical applications, Tokamak device [7] for nuclear fusion, an intangible doughnut-shaped bottle created by magnetic lines is used to confine the high-temperature plasma, as well as air traffic flow in the National Airspace System [8], steam-jacket tubular heat exchanger [4,9,10], etc. These spatially distributed processes (SDPs) are naturally described by a set of nonlinear partial differential equations (PDEs) with homogeneous or mixed boundary conditions. Moreover, there inevitably exist some kinds of external disturbances impinging on the processes. Therefore, studying the disturbance attenuation control problem of nonlinear PDE systems is of theoretical and practical importance.

For nonlinear systems described by ordinary differential equations (ODEs), an effective solution is to address the problem of disturbance attenuation in the L_2-gain (H_∞ norm) setting [11–13], that is, to design a controller such that the ratio of the objective output energy to the disturbance energy is less than a prescribed level. Over the past few decades, a large number of theoretical results on nonlinear H_∞ control have been reported [14–17], where the H_∞ controller depends on the solution of the so-called Hamilton–Jacobi–Isaacs (HJI) equation. The HJI equation is a first order nonlinear PDE, which is difficult or impossible to solve, and may not have global analytic solutions even in simple cases. Thus, some works have been done in recent years to approximately obtain the solution of the HJI equation [14,18–20]. In [14], it was shown that there exists a sequence of policy iterations on the control input to pursue the smooth solution of the HJI equation, where a sequence of Hamilton-Jacobi-Bellman (HJB)-like equations were used to successively approximate the HJI equation. In

* Corresponding author. Tel.: +86 1082317301; fax: +86 1082317332.
E-mail addresses: whn@buaa.edu.cn, huainingwu@163.com (H.-N. Wu).

http://dx.doi.org/10.1016/j.jprocont.2014.02.017
0959-1524/© 2014 Elsevier Ltd. All rights reserved.

Author's personal copy

this way, the methods for solving HJB equation can be extended for the solution of HJI equation. In [21], the HJB equation was successively approximated by a sequence of linear PDEs, which were solved with Galerkin's approximation in [22,23]. Inspired by [14,21,22], Beard and Mclain [19] further successively approximated each HJB-like equation in [14] with a sequence of linear PDEs, and then solved by Galerkin's approximation. This results in two iterative loops, i.e., the inner loop solves a HJB-like equation by iteratively solving a sequence of linear PDEs, and the outer loop solves the HJI equation by iteratively solving a sequence of HJB-like equations. Thus, Luo and Wu [20] proposed a more efficient simultaneous policy update algorithm (SPUA), in which the HJI equation is solved by iteratively solving a sequence of linear PDEs, and then only one iterative loop is required.

Due to the infinite-dimensional nature of the PDE systems, it is very difficult to directly use the control design methods of ODE systems for the SDPs. To achieve the disturbance attenuation, some control design approaches for SDPs with external disturbances have been proposed, such as, infinite-dimensional H_∞ control method [24], H_∞ fuzzy control methods [25–28] and neural network based L_∞-gain control method [29]. The infinite-dimensional H_∞ control method in [24] analyzes the PDE systems in an infinite-dimensional abstract space and leads to an infinite-dimensional controller that is difficult to implement in practice; Furthermore, this method is mainly limited to linear systems, and not suitable for nonlinear PDE systems. The methods in [26–29] were developed for nonlinear PDE systems with linear spatial differential operator, which are not applied to PDE systems with nonlinear spatial differential operator; moreover, the linear matrix inequality (LMI) techniques are employed in [25–29], which often bring conservatisms. However, to the best of the authors' knowledge, the L_2 disturbance attenuation problem of a general class of highly dissipative SDPs is rarely studied in the framework of HJI equations.

In this work, we develop a SPUA based HJI approach to solve the L_2 disturbance attenuation problem of a general class of highly dissipative nonlinear PDE systems. Initially, we use the Karhunen-Loève decomposition (KLD) to compute EEFs for the SDP with the method of snapshots. These empirical eigenfunctions (EEFs) together with singular perturbation (SP) technique are subsequently used to obtain a finite-dimensional slow subsystem that accurately describes the dominant dynamics of the PDE system. Then, based on the slow subsystem, the L_2 disturbance attenuation problem is reformulated, and solved in terms of the HJI equation. Moreover, the stability and L_2-gain performance of the closed-loop PDE system are analyzed. Furthermore, we introduce the SPUA to solve the HJI equation, which is successively approximated by a sequence of linear PDEs and solved with the method of weighted residuals (MWR). Finally, the simulation studies on a nonlinear diffusion-reaction process and a temperature cooling fin of high-speed aerospace vehicle are given to show the effectiveness of the proposed design method.

The rest of this paper is arranged as follows. The problem description is given in Section 2 and the L_2 disturbance attenuation problem is reformulated using the EEFs and the SP technique in Section 3. Section 4 presents the HJI approach for designing the H_∞ control law and Section 5 shows the simulation results. Finally, a brief conclusion is drawn in Section 6.

Notations: $\mathbb{R}$, $\mathbb{R}^n$ and $\mathbb{R}^{n\times m}$ are the set of real numbers, the n-dimensional Euclidean space and the set of all real $n\times m$ matrices, respectively. $|\cdot|$, $||\cdot||$, and $\langle\cdot,\cdot\rangle_{\mathbb{R}^n}$ stand for the absolute value for scalars, Euclidean norm and inner product for vectors, respectively. Let $\mathbb{R}^\infty$ be the vector space of infinite sequences $\boldsymbol{\alpha}\triangleq[\alpha_1\cdots\alpha_\infty]^T$ of real numbers equipped with the norm $||\boldsymbol{\alpha}||_{\mathbb{R}^\infty}\triangleq\sqrt{\sum_{i=1}^{\infty}\alpha_i^2}$, which is a natural generalization of $\mathbb{R}^n$. Identity matrix, of appropriate dimensions, is denoted by $\boldsymbol{I}$. The superscript 'T' is used for the transpose of a vector or a matrix. $\bar{\sigma}(\cdot)$, $\underline{\sigma}(\cdot)$ and $\bar{\lambda}$ denote the maximum singular value, the minimum singular value and the maximum eigenvalue of a matrix. For a symmetric matrix $\boldsymbol{M}$, $\boldsymbol{M}>(\ge,<,\le)0$ means that it is positive definite (positive semi-definite, negative definite, negative semi-definite, respectively). The space-varying symmetric matrix function $\boldsymbol{M}(z)$, $z\in[\underline{z},\bar{z}]$ is positive definite (positive semi-definite, negative definite, negative semi-definite, respectively), if $\boldsymbol{M}(z)>(\ge,<,\le)0$ for each $z\in[\underline{z},\bar{z}]$. For column vector functions $\boldsymbol{s}_1(\boldsymbol{x})$ and $\boldsymbol{s}_2(\boldsymbol{x})$, define inner product $\langle\boldsymbol{s}_1(\cdot),\boldsymbol{s}_2(\cdot)\rangle_\Omega\triangleq\int_\Omega\boldsymbol{s}_1^T(\boldsymbol{x})\boldsymbol{s}_2(\boldsymbol{x})d\boldsymbol{x}$, $\boldsymbol{x}\in\Omega\subset\mathbb{R}^n$. $\mathscr{L}_2([\underline{z},\bar{z}];\mathbb{R}^n)$ is an infinite-dimensional Hilbert space of n-dimensional square integrable vector functions $\boldsymbol{\omega}(z)\in\mathscr{L}_2([\underline{z},\bar{z}];\mathbb{R}^n)$, $z\in[\underline{z},\bar{z}]\subset\mathbb{R}$ equipped with the inner product and norm: $\langle\boldsymbol{\omega}_1(\cdot),\boldsymbol{\omega}_2(\cdot)\rangle=\int_{\underline{z}}^{\bar{z}}\langle\boldsymbol{\omega}_1(z),\boldsymbol{\omega}_2(z)\rangle_{\mathbb{R}^n}dz$ and $||\boldsymbol{\omega}_1(\cdot)||_2=\langle\boldsymbol{\omega}_1(\cdot),\boldsymbol{\omega}_1(\cdot)\rangle^{1/2}$ where $\boldsymbol{\omega}_1(\cdot)$ and $\boldsymbol{\omega}_2(\cdot)$ are any two elements of $\mathscr{L}_2([\underline{z},\bar{z}],\mathbb{R}^n)$.

2. Problem description

We consider a general class of continuous-time SDPs which are described by highly dissipative nonlinear PDEs with the following state-space representation:

$$\begin{cases}\dfrac{\partial\boldsymbol{y}}{\partial t}=\mathscr{L}\left(\boldsymbol{y},\dfrac{\partial\boldsymbol{y}}{\partial z},\dfrac{\partial^2\boldsymbol{y}}{\partial z^2},\ldots,\dfrac{\partial^{n_0}\boldsymbol{y}}{\partial z^{n_0}}\right)+\bar{\boldsymbol{B}}_1(z)\boldsymbol{w}(t)+\bar{\boldsymbol{B}}_2(z)\boldsymbol{u}(t)\\ \boldsymbol{y}_h(t)=\displaystyle\int_{\underline{z}}^{\bar{z}}\boldsymbol{H}(z)\boldsymbol{y}(z,t)dz\end{cases}\tag{1}$$

subject to the mixed-type boundary conditions

$$\boldsymbol{q}\left(\boldsymbol{y},\frac{\partial\boldsymbol{y}}{\partial z},\frac{\partial^2\boldsymbol{y}}{\partial z^2},\cdots,\frac{\partial^{n_0-1}\boldsymbol{y}}{\partial z^{n_0-1}}\right)\Bigg|_{z=\underline{z}\ \text{or}\ \bar{z}}=0\tag{2}$$

and the initial condition

$$\boldsymbol{y}(z,0)=\boldsymbol{y}_0(z)\tag{3}$$

where $z\in[\underline{z},\bar{z}]\subset\mathbb{R}$ is the spatial coordinate, $t\in[0,\infty)$ is the temporal coordinate, $\boldsymbol{y}(z,t)=[y_1(z,t)\cdots y_n(z,t)]^T\in\mathbb{R}^n$ is the state, $\boldsymbol{u}(t)\in\mathbb{R}^p$ is the manipulated input, $\boldsymbol{y}_h(t)=\begin{bmatrix}y_{h,1}(t) & \cdots & y_{h,m}(t)\end{bmatrix}^T\in\mathbb{R}^m$ is the objective output, $\boldsymbol{w}(t)\in\mathbb{R}^q$ is the exogenous disturbance and $\boldsymbol{w}(t)\in\mathscr{L}_2([0,\infty),\mathbb{R}^q)$. $\mathscr{L}\in\mathbb{R}^n$ is a sufficiently smooth nonlinear vector function that involves a highly dissipative, possibly nonlinear, spatial differential operator of order n_0 (an even number). $\boldsymbol{q}$ is a sufficiently smooth nonlinear vector function. $\bar{\boldsymbol{B}}_1(z)$ and $\bar{\boldsymbol{B}}_2(z)$ are sufficiently smooth matrix functions of appropriate dimensions which describe how disturbance and control actions are distributed in spatial domains respectively, $\boldsymbol{H}(z)$ is a selected sufficiently smooth matrix function of appropriate dimension, and $\boldsymbol{y}_0(z)$ is a smooth vector function representing the initial state profile.

Author's personal copy

Remark 1. The highly dissipative nonlinear PDE system (1)–(3) represents a large number of nonlinear industrial SDPs. Representative examples include transport-reaction processes with significant diffusive and dispersive mechanisms that are naturally described by nonlinear parabolic PDEs (such as chemical reactors [4,30,31], catalytic rod [1,2,4,29], heat transfer [32], chemical vapor deposition [4,5], crystal growth processes [3], FitzHugh–Nagumo equation [33], etc.), and several fluid dynamic systems (such as Burgers's equation [34] for gas dynamics and traffic flow, Kuramoto–Sivashinsky equation (KSE) [1,33,35], Navier–Stokes equations [35], etc.).

The L_2 disturbance attenuation problem under consideration is to find a state feedback control law such that the system (1)–(3) has L_2-gain less than or equal to γ, that is,

$$\int_0^{+\infty}(||\boldsymbol{y}_h(t)||^2+\boldsymbol{u}^T(t)\boldsymbol{R}\boldsymbol{u}(t))dt \le \gamma^2\int_0^{+\infty}||\boldsymbol{w}(t)||^2dt \tag{4}$$

for all $\boldsymbol{w}(\mathrm{t})\in\mathscr{L}_2([0,\infty),\mathbb{R}^q)$, (i.e., $\int_0^{+\infty}||\boldsymbol{w}(t)||^2\,dt<\infty$), where $\boldsymbol{R}\geq 0$ is the given weighting matrix and $\gamma>0$ is some prescribed level of disturbance attenuation.

3. Finite-dimensional L_2 disturbance attenuation problem formulation

It is known that the main feature of highly dissipative PDE systems is that they involve spatial differential operators whose eigenspectrum can be partitioned into a finite-dimensional slow one and an infinite-dimensional stable fast complement. This means that their dominant dynamic behavior can be accurately described by finite-dimensional systems. However, for many real industrial SDPs with nonlinear spatial differential operators [1,5,36–39], it is impossible to compute their analytic expressions of the eigenvalues and eigenfunctions, and thus, the direct use of basis functions are prohibited to derive finite-dimensional approximations of the PDE system. To overcome this difficulty, we initially compute a set of EEFs (dominant spatial patterns) of the PDE system by using KLD based on the method of snapshots. These EEFs together with the SP technique will be subsequently applied to obtain a slow subsystem that accurately describes the dominant dynamics of the PDE system. Then, the L_2 disturbance attenuation problem is reformulated on the basis of the slow subsystem, which is prepared for synthesizing a finite-dimensional H_∞ controller.

3.1. Computation of EEFs with KLD

KLD is a popular statistical pattern analysis method for seeking the dominant structures in an ensemble of a high-dimensional process, and obtaining low-dimensional approximate descriptions in many engineering fields. Given an ensemble of data, KLD yields a set of orthogonal EEFs for the representation of the ensemble, as well as a measure of the relative contribution of each EEF to the total "energy" (mean square fluctuation) of the ensemble. In this sense, the EEFs provide an optimal basis for the truncated series representation, which has a smaller mean square error than a representation by any other basis of the same dimension. In other words, the projection onto the first few EEFs captures most of the energy than any other projection. These properties make the EEFs a natural one to be considered when performing model reduction.

For completeness sake, we briefly review the procedure of KLD for computing EEFs with the method of snapshots in the context of the PDE system (1)–(3). By using different initial conditions, control inputs and disturbances, conduct simulations on the SDP and online collect a representative ensemble $\{\boldsymbol{y}_i(z)\}$. The ensemble is a set with the size M that is sufficiently large, and $\boldsymbol{y}_i(z)$ is typically called "snapshot" of the solution of the PDE system. Introduce the two-point spatial correlation function as

$$\boldsymbol{S}(z,\xi)=\frac{1}{M}\sum_{i=1}^{M}\boldsymbol{y}_i(z)\boldsymbol{y}_i^T(\xi) \tag{6}$$

According to the Mercer theorem [40], $\boldsymbol{S}(z,\xi)$ has a property that

$$\boldsymbol{S}(z,\xi)=\sum_{j=1}^{\infty}\lambda_j\boldsymbol{\phi}_j(z)\boldsymbol{\phi}_j^T(\xi) \tag{7}$$

where $\{\lambda_j\}$ is the set of non-zero eigenvalues and $\{\boldsymbol{\phi}_j(z)\}$ is the corresponding set of orthogonal eigenfunctions of $\boldsymbol{S}(z,\xi)$.By using Eq. (6), we have

$$\begin{aligned}\int_{\underline{z}}^{\bar{z}}\boldsymbol{S}(z,\xi)\boldsymbol{\phi}_i(\xi)d\xi &= \int_{\underline{z}}^{\bar{z}}\frac{1}{M}\sum_{j=1}^{M}\boldsymbol{y}_j(z)\boldsymbol{y}_j^T(\xi)\boldsymbol{\phi}_i(\xi)d\xi\\ &=\sum_{j=1}^{M}\boldsymbol{y}_j(z)\left[\frac{1}{M}\int_{\underline{z}}^{\bar{z}}\boldsymbol{y}_j^T(\xi)\boldsymbol{\phi}_i(\xi)d\xi\right]=\sum_{j=1}^{M}\vartheta_j y_j(z)\end{aligned} \tag{8}$$

where $\vartheta_j=\frac{1}{M}\int_{\underline{z}}^{\bar{z}}\boldsymbol{y}_j^T(\xi)\boldsymbol{\phi}_i(\xi)d\xi$. Similarly, by using (7), we get

$$\begin{aligned}\int_{\underline{z}}^{\bar{z}}\boldsymbol{S}(z,\xi)\boldsymbol{\phi}_i(\xi)d\xi &= \int_{\underline{z}}^{\bar{z}}\sum_{j=1}^{\infty}\lambda_j\boldsymbol{\phi}_j(z)\boldsymbol{\phi}_j^T(\xi)\boldsymbol{\phi}_i(\xi)d\xi\\ &=\sum_{j=1}^{\infty}\lambda_j\boldsymbol{\phi}_j(z)\int_{\underline{z}}^{\bar{z}}\boldsymbol{\phi}_j^T(\xi)\boldsymbol{\phi}_i(\xi)d\xi=\lambda_i\boldsymbol{\phi}_i(z)\end{aligned} \tag{9}$$

Author's personal copy

It follows from (8) and (9) that

$$\boldsymbol{\phi}_i(z) = \sum_{j=1}^{M} \alpha_{ji} \boldsymbol{y}_j(z) \tag{10}$$

where $\alpha_{ji} \triangleq \lambda_i^{-1} \vartheta_j$. This means that the EEFs $\{\boldsymbol{\phi}_i(z)\}$ are linear combinations of snapshots $\{\boldsymbol{y}_i(z)\}$. Then, the essence of computing EEFs is reduced to compute the coefficient vectors $\boldsymbol{\alpha}_i = [\alpha_{1i} \cdots \alpha_{Mi}]^T$.

The substitution of expressions (6) and (10) into (9) yields

$$\int_{\underline{z}}^{\bar{z}} \frac{1}{M} \sum_{k=1}^{M} \boldsymbol{y}_k(z) \boldsymbol{y}_k^T(\xi) \sum_{j=1}^{M} \alpha_{ji} \boldsymbol{y}_j(\xi) d\xi = \lambda_i \sum_{j=1}^{M} \alpha_{ji} \boldsymbol{y}_j(z)$$

i.e.,

$$\sum_{k=1}^{M} \boldsymbol{y}_k(z) \sum_{j=1}^{M} \alpha_{ji} \left[\frac{1}{M} \int_{\underline{z}}^{\bar{z}} \boldsymbol{y}_k^T(\xi) \boldsymbol{y}_j(\xi) d\xi \right] = \lambda_i \sum_{j=1}^{M} \alpha_{ji} \boldsymbol{y}_j(z)$$

then, we get

$$\boldsymbol{Y}(z)(\boldsymbol{C}\boldsymbol{\alpha}_i) = \boldsymbol{Y}(z)(\lambda_i \boldsymbol{\alpha}_i) \tag{11}$$

where $\boldsymbol{C} = (c_{kj})_{M \times M} \in \mathbb{R}^{M \times M}$ and $\boldsymbol{Y}(z) = [\boldsymbol{y}_1(z) \cdots \boldsymbol{y}_M(z)] \in \mathbb{R}^{n \times M}$ with

$$c_{kj} = \frac{1}{M} \int_{\underline{z}}^{\bar{z}} \boldsymbol{y}_k^T(\xi) \boldsymbol{y}_j(\xi) d\xi$$

Assuming that $\{\boldsymbol{y}_i(z)\}$ are linearly independent, all eigenvectors $\{\boldsymbol{\alpha}_i\}$ and corresponding eigenvalues $\{\lambda_i\}$ can be computed by the standard method of eigenvalue decomposition for the following eigenvalue problem:

$$\boldsymbol{C}\boldsymbol{\alpha}_i = \lambda_i \boldsymbol{\alpha}_i.$$

EEFs can be mutually orthogonal by normalizing the eigenvector α_i to satisfy

$$\langle \boldsymbol{\alpha}_i, \boldsymbol{\alpha}_i \rangle_{\mathbb{R}^n} = \frac{1}{M\lambda_i}$$

Then, all EEFs $\{\boldsymbol{\phi}_i(z)\}$ are directly computed by (10).

3.2. *Problem formulation of finite-dimensional L_2 disturbance attenuation*

For convenience, we denote $\boldsymbol{y}(\cdot, t) \triangleq \boldsymbol{y}(z, t)$, $z \in [\underline{z}, \bar{z}]$ and $\boldsymbol{M}(\cdot) \triangleq \boldsymbol{M}(z)$, $z \in [\underline{z}, \bar{z}]$ for some space-varying matrix function $\boldsymbol{M}(z)$. To simplify the notation, we consider the PDE system (1)–(3) with $n = 1$ without loss of generality. Assume that the PDE state $y(z, t)$ can be represented as an infinite weighted sum of a complete set of orthogonal basis functions $\{\phi_i(z)\}$, i.e.,

$$y(z, t) = \sum_{i=1}^{\infty} x_i(t) \phi_i(z) \tag{12}$$

where $x_i(t)$ is a time-varying coefficient named the mode of the PDE system. By taking inner product with $\phi_i(z)$ $(i = 1, \ldots)$ on both sides of PDE system (1)–(3), we obtain the following infinite-dimensional ODE system:

$$\begin{cases} \dot{\boldsymbol{x}}(t) = \boldsymbol{f}_s(\boldsymbol{x}(t), \boldsymbol{x}_f(t)) + \boldsymbol{B}_1 \boldsymbol{w}(t) + \boldsymbol{B}_2 \boldsymbol{u}(t) \\ \dot{\boldsymbol{x}}_f(t) = \mathscr{L}_f(\boldsymbol{x}(t), \boldsymbol{x}_f(t)) + \boldsymbol{B}_{1f} \boldsymbol{w}(t) + \boldsymbol{B}_{2f} \boldsymbol{u}(t) \\ \boldsymbol{y}_h(t) = \boldsymbol{H}_s \boldsymbol{x}(t) + \boldsymbol{H}_f \boldsymbol{x}_f(t) \\ \boldsymbol{x}(0) = \boldsymbol{x}_0, \boldsymbol{x}_f(0) = \boldsymbol{x}_{f0} \end{cases} \tag{13}$$

where

$$\boldsymbol{x}(t) = \left\langle y(\cdot, t), \boldsymbol{\Phi}_s(\cdot) \right\rangle \triangleq [x_1(t) \cdots x_N(t)]^T \tag{14}$$

and

$$\boldsymbol{x}_f(t) = \langle y(\cdot, t), \boldsymbol{\Phi}_f(\cdot) \rangle \triangleq [x_{N+1}(t) \cdots x_\infty(t)]^T \in \mathbb{R}^\infty$$
$$\boldsymbol{f}_s(\boldsymbol{x}, \boldsymbol{x}_f) \triangleq \langle \mathscr{L}, \boldsymbol{\Phi}_s(\cdot) \rangle, \mathscr{L}_f(\boldsymbol{x}, \boldsymbol{x}_f) \triangleq \langle \mathscr{L}, \boldsymbol{\Phi}_f(\cdot) \rangle$$
$$\boldsymbol{B}_1 \triangleq \langle \bar{\boldsymbol{B}}_1(\cdot), \boldsymbol{\Phi}_s(\cdot) \rangle, \boldsymbol{B}_{1f} \triangleq \langle \bar{\boldsymbol{B}}_1(\cdot), \boldsymbol{\Phi}_f(\cdot) \rangle, \boldsymbol{B}_2 \triangleq \langle \bar{\boldsymbol{B}}_2(\cdot), \boldsymbol{\Phi}_s(\cdot) \rangle, \boldsymbol{B}_{2f} \triangleq \langle \bar{\boldsymbol{B}}_2(\cdot), \boldsymbol{\Phi}_f(\cdot) \rangle$$
$$\boldsymbol{H}_s \triangleq \int_{\underline{z}}^{\bar{z}} \boldsymbol{H}(z) \boldsymbol{\Phi}_s^T(z) dz, \boldsymbol{H}_f \triangleq \int_{\underline{z}}^{\bar{z}} \boldsymbol{H}(z) \boldsymbol{\Phi}_f^T(z) dz$$
$$\boldsymbol{x}_0 \triangleq \langle \boldsymbol{y}_0(\cdot), \boldsymbol{\Phi}_s(\cdot) \rangle, \boldsymbol{x}_{f0} \triangleq \langle \boldsymbol{y}_0(\cdot), \boldsymbol{\Phi}_f(\cdot) \rangle$$

Author's personal copy

with $\boldsymbol{\Phi}_s(z) \triangleq [\phi_1(z) \cdots \phi_N(z)]^T$ and $\boldsymbol{\Phi}_f(z) \triangleq [\phi_{N+1}(z) \cdots \phi_\infty(z)]^T$ Similarly, the L_2 disturbance attenuation criterion (4) is rewritten as

$$\int_0^{+\infty} (\boldsymbol{x}^T(t)\boldsymbol{Q}_s\boldsymbol{x}(t) + \boldsymbol{u}^T(t)\boldsymbol{R}\boldsymbol{u}(t))dt + \Re(\boldsymbol{x}, \boldsymbol{x}_f) \le \gamma^2 \int_0^{+\infty} ||\boldsymbol{w}(t)||^2\, dt \tag{15}$$

where $\Re(\boldsymbol{x}, \boldsymbol{x}_f) \triangleq \int_0^{+\infty} (2\boldsymbol{x}^T(t)\boldsymbol{Q}_{sf}\boldsymbol{x}_f(t) + \boldsymbol{x}_f^T(t)\boldsymbol{Q}_f\boldsymbol{x}_f(t))dt$, $\boldsymbol{Q}_s \triangleq \boldsymbol{H}_s^T\boldsymbol{H}_s$, $\boldsymbol{Q}_{sf} \triangleq \boldsymbol{H}_s^T\boldsymbol{H}_f$ and $\boldsymbol{Q}_f \triangleq \boldsymbol{H}_f^T\boldsymbol{H}_f$

Assumption 1. There exist constants $\alpha_1, \gamma_f > 0$ such that the following inequality holds

$$\Re(\boldsymbol{x}, \boldsymbol{x}_f) \le \alpha_1 \int_0^{+\infty} (\boldsymbol{x}^T(t)\boldsymbol{Q}_s\boldsymbol{x}(t) + \boldsymbol{u}^T(t)\boldsymbol{R}\boldsymbol{u}(t))dt + \gamma_f^2 \int_0^{+\infty} ||\boldsymbol{w}(t)||^2\, dt \tag{16}$$

Owing to the highly dissipative nature of the PDE system (1)–(3), it is reasonable to assume that

$$\mathscr{L}_f(\boldsymbol{x}, \boldsymbol{x}_f) = \frac{1}{\varepsilon}\boldsymbol{A}_{f\varepsilon}\boldsymbol{x}_f + \boldsymbol{f}_f(\boldsymbol{x}, \boldsymbol{x}_f) \tag{17}$$

where ε is a small positive parameter quantifying the separation between the slow (dominant) and fast (negligible) modes, $A_{f\varepsilon}$ is a matrix that is stable (in the sense that the state of the system $\dot{\boldsymbol{x}}_f = \boldsymbol{A}_{f\varepsilon}\boldsymbol{x}_f$ tends exponentially to zero), and $\boldsymbol{f}_f(\boldsymbol{x}, \boldsymbol{x}_f)$ satisfies

$$||\boldsymbol{f}_f(\boldsymbol{x}, \boldsymbol{x}_f)|| \le k_1||\boldsymbol{x}|| + k_2||\boldsymbol{x}_f|| \tag{18}$$

for $||\boldsymbol{x}|| \le \beta_1$ and $||\boldsymbol{x}_f|| \le \beta_2$ with $k_1, k_2 > 0$. Then, system (13) can be rewritten as the following standard singularly perturbed form:

$$\begin{cases} \dot{\boldsymbol{x}}(t) = \boldsymbol{f}_s(\boldsymbol{x}(t), \boldsymbol{x}_f(t)) + \boldsymbol{B}_1\boldsymbol{w}(t) + \boldsymbol{B}_2\boldsymbol{u}(t) \\ \varepsilon\dot{\boldsymbol{x}}_f(t) = \boldsymbol{A}_{f\varepsilon}\boldsymbol{x}_f(t) + \varepsilon\boldsymbol{f}_f(\boldsymbol{x}(t), \boldsymbol{x}_f(t)) + \varepsilon\boldsymbol{B}_{1f}\boldsymbol{w}(t) + \varepsilon\boldsymbol{B}_{2f}\boldsymbol{u}(t) \\ \boldsymbol{y}_h(t) = \boldsymbol{H}_s\boldsymbol{x}(t) + \boldsymbol{H}_f\boldsymbol{x}_f(t) \\ \boldsymbol{x}(0) = \boldsymbol{x}_0, \boldsymbol{x}_f(0) = \boldsymbol{x}_{f0} \end{cases} \tag{19}$$

Introducing the fast time-scale $\tau = t/\varepsilon$ and setting $\varepsilon = 0$, we obtain the following infinite-dimensional fast subsystem from (19):

$$\frac{d\boldsymbol{x}_f}{d\tau} = \boldsymbol{A}_{f\varepsilon}\boldsymbol{x}_f \tag{20}$$

which is exponentially stable [37,41]. Then, setting $\varepsilon = 0$ in the system (19), we have $\boldsymbol{x}_f = 0$, and thus the following slow subsystem is obtained:

$$\begin{cases} \dot{\boldsymbol{x}}(t) = \boldsymbol{f}_s(\boldsymbol{x}(t), 0) + \boldsymbol{B}_1\boldsymbol{w}(t) + \boldsymbol{B}_2\boldsymbol{u}(t), \quad \boldsymbol{x}(0) = \boldsymbol{x}_0 \\ \boldsymbol{y}_{hs}(t) = \boldsymbol{H}_s\boldsymbol{x}(t) \end{cases} \tag{21}$$

The basis function $\phi_i(z)$ used in this paper is the EEF computed with KLD, and the dimension of $\boldsymbol{\Phi}_s$ (i.e., N) is chosen such that it satisfies

$$\sum_{i=1}^{N}\lambda_i \Big/ \sum_{i=1}^{M}\lambda_i \ge 1 - \zeta \tag{22}$$

for a small positive real number ζ.

In this study, the slow subsystem (21) will be used as the basis for synthesizing a finite-dimensional H_∞ controller for PDE system (1)–(3) such that the following L_2 disturbance attenuation criterion is satisfied:

$$\int_0^{+\infty} (\boldsymbol{x}^T(t)\boldsymbol{Q}_s\boldsymbol{x}(t) + \boldsymbol{u}^T(t)\boldsymbol{R}\boldsymbol{u}(t))dt \le \gamma_s^2 \int_0^{+\infty} ||\boldsymbol{w}(t)||^2\, dt \tag{23}$$

where γ_s is a given positive constant satisfying $0 < \gamma_s < \gamma$.

Remark 2. Compared with analytical eigenfunctions, the use of EEFs for model reduction of nonlinear PDE systems has two merits. The first is that analytical eigenfunctions are only suitable to set up a finite dimensional ODE system for PDE systems with a known linear spatial differential operator. However, EEFs are suitable for the model reduction of PDE systems with nonlinear spatial differential operator. Another important merit of EEFs is that they can be computed online on the basis of data collection of system states by using KLD, which does not require a mathematical system model. Thus, the highly-complexity and unavailability of internal system dynamic $\mathscr{L}$ have no effects on the computation of EEFs.

4. HJI approach for finite-dimensional H_∞ control design

To synthesize a finite-dimensional H_∞ controller for the PDE system (1)–(3), it is well known that, the L_2 disturbance attenuation problem for the finite-dimensional nonlinear ODE system (21) with the L_2-gain performance (23), can be converted to solve a HJI equation [12,13]. However, HJI equation is notoriously difficult to solve both numerically and analytically. To overcome this difficulty, we combine the SPUA and MWR to approximately solve the HJI equation.

Author's personal copy

4.1. HJI approach and stability analysis

The following Lemma 1 shows that the L_2 disturbance attenuation problem of ODE system (21) with the L_2-gain performance (23) is translated to solve a HJI equation for value function.

Lemma 1. Consider the slow system (21) and the L_2-gain performance (23). Assume that the system is zero-state observable. If there exists a smooth solution $V^*(\boldsymbol{x})\geq 0$ to the HJI equation

$$(\nabla V^*(\boldsymbol{x}))^T\boldsymbol{f}_s(\boldsymbol{x},0)+\boldsymbol{x}^T\boldsymbol{Q}_s\boldsymbol{x}-\frac{1}{4}(\nabla V^*(\boldsymbol{x}))^T\boldsymbol{B}_2\boldsymbol{R}^{-1}\boldsymbol{B}_2^T\nabla V^*(\boldsymbol{x})+\frac{1}{4\gamma_s^2}(\nabla V^*(\boldsymbol{x}))^T\boldsymbol{B}_1\boldsymbol{B}_1^T\nabla V^*(\boldsymbol{x})=0 \tag{24}$$

where $\nabla\triangleq\partial/\partial x$ is a gradient operator notation, then, the closed-loop system with the state feedback control

$$\boldsymbol{u}(t)=\boldsymbol{u}^*(\boldsymbol{x})=-\frac{1}{2}\boldsymbol{R}^{-1}\boldsymbol{B}_2^T\nabla V^*(\boldsymbol{x}) \tag{25}$$

has L_2-gain less than or equal to γ_s (i.e., (23) holds), and is locally asymptotically stable (when $\boldsymbol{w}(t)\equiv 0$).

Proof. See Theorem 16 and Corollary 17 in [14].

Notice that the modal feedback control policy (25) in Lemma 1 only shows the stability and the L_2-gain performance of the closed-loop slow system; nothing about the original closed-loop PDE system is analyzed. Next, we will prove that under the control policy (25), the closed-loop PDE system of (1)–(3) is also locally asymptotically stable (when $\boldsymbol{w}(t)\equiv 0$) and satisfies the original L_2-gain criterion (4).

Theorem 1. Consider the PDE system (1)–(3) and the L_2 disturbance attenuation criterion (4), for which Assumption 1 holds with constants $\alpha_1,\gamma_f>0$, the conditions of Lemma 1 hold, and give constant γ_s. Then, with the modal feedback control policy (25), there exist positive real constants γ, δ_1, δ_2 and ε^*, such that if $\|\boldsymbol{x}_0\|\leq\delta_1$, $\|\boldsymbol{x}_{f0}\|_{\mathbb{R}^\infty}\leq\delta_2$ and $\varepsilon\in(0,\varepsilon^*)$,

(1) the closed-loop PDE system (1)–(3) has L_2-gain less than or equal to γ (i.e., (4) holds) for all $\boldsymbol{w}(t)\in\mathscr{L}_2([0,\infty),\mathbb{R}^q)$, where $\gamma\geq\sqrt{(1+\alpha_1)\gamma_s^2+\gamma_f^2}$
(2) the disturbance-free closed-loop PDE system (1)–(3) (i.e., $\boldsymbol{w}(t)\equiv 0$) is locally asymptotically stable in $\mathscr{L}_2$-norm.

Proof. Under the modal feedback control policy (25), it follows from Lemma 1 and Assumption 1 that inequalities (16) and (23) hold. Then, by using (16) and (23), we get

$$\begin{aligned}
&\int_0^{+\infty}(\boldsymbol{x}^T(t)\boldsymbol{Q}_s\boldsymbol{x}(t)+\boldsymbol{u}^{*T}(t)\boldsymbol{R}\boldsymbol{u}^*(t))dt+\Re(\boldsymbol{x},\boldsymbol{x}_f)\\
&\leq\gamma_s^2\int_0^{+\infty}\|\boldsymbol{w}(t)\|^2\,dt+\alpha_1\left(\int_0^{+\infty}(\boldsymbol{x}^T(t)\boldsymbol{Q}_s\boldsymbol{x}(t)+\boldsymbol{u}^{*T}(t)\boldsymbol{R}\boldsymbol{u}^*(t))dt\right)+\gamma_f^2\int_0^{+\infty}\|\boldsymbol{w}(t)\|^2\,dt\\
&\leq(\gamma_s^2+\gamma_f^2)\int_0^{+\infty}\|\boldsymbol{w}(t)\|^2\,dt+\alpha_1\left(\int_0^{+\infty}(\boldsymbol{x}^T(t)\boldsymbol{Q}_s\boldsymbol{x}(t)+\boldsymbol{u}^{*T}(t)\boldsymbol{R}\boldsymbol{u}^*(t))dt\right)\\
&\leq(\gamma_s^2+\gamma_f^2)\int_0^{+\infty}\|\boldsymbol{w}(t)\|^2\,dt+\alpha_1\gamma_s^2\int_0^{+\infty}\|\boldsymbol{w}(t)\|^2\,dt\\
&=((1+\alpha_1)\gamma_s^2+\gamma_f^2)\int_0^{+\infty}\|\boldsymbol{w}(t)\|^2\,dt
\end{aligned}$$

Since $\gamma\geq\sqrt{(1+\alpha_1)\gamma_s^2+\gamma_f^2}$, we have

$$\begin{aligned}
&\int_0^{+\infty}(\|\boldsymbol{y}_h(t)\|^2+\boldsymbol{u}^{*T}(t)\boldsymbol{R}\boldsymbol{u}^*(t))dt=\int_0^{+\infty}\left(\boldsymbol{x}^T(t)\boldsymbol{Q}_s\boldsymbol{x}(t)+\boldsymbol{u}^{*T}(t)\boldsymbol{R}\boldsymbol{u}^*(t)\right)dt+\Re(\boldsymbol{x},\boldsymbol{x}_f)\\
&\leq\gamma^2\int_0^{+\infty}\|\boldsymbol{w}(t)\|^2\,dt
\end{aligned}$$

This means that the closed-loop PDE system (1)–(3) with the control policy (25) satisfies the L_2 disturbance attenuation criterion (4).

In addition, with the control policy (25), the disturbance-free closed-loop PDE system is given by

$$\frac{\partial\boldsymbol{y}}{\partial t}=\mathscr{L}\left(\boldsymbol{y},\frac{\partial\boldsymbol{y}}{\partial z},\frac{\partial^2\boldsymbol{y}}{\partial z^2},\cdots,\frac{\partial^{n_0}\boldsymbol{y}}{\partial z^{n_0}}\right)+\bar{\boldsymbol{B}}_2(z)\boldsymbol{u}^*(t) \tag{26}$$

Using the procedure given in Section 3.2, the system (26) is equivalently represented as

$$\begin{cases}\dot{\boldsymbol{x}}=\boldsymbol{f}_s(\boldsymbol{x},0)+\boldsymbol{B}_2\boldsymbol{u}^*+(\boldsymbol{f}_s(\boldsymbol{x},\boldsymbol{x}_f)-\boldsymbol{f}_s(\boldsymbol{x},0))\\ \varepsilon\dot{\boldsymbol{x}}_f=\boldsymbol{A}_{f\varepsilon}\boldsymbol{x}_f+\varepsilon\boldsymbol{f}_f(\boldsymbol{x},\boldsymbol{x}_f)+\varepsilon\boldsymbol{B}_{2f}\boldsymbol{u}^*\end{cases} \tag{27}$$

Since $\mathscr{L}$ is a sufficiently smooth nonlinear vector function, it is obvious that there exists some constant $k_3>0$ such that

$$\|\boldsymbol{f}_s(\boldsymbol{x},\boldsymbol{x}_f)-\boldsymbol{f}_s(\boldsymbol{x},0)\|\leq k_3\|\boldsymbol{x}_f\|_{\mathbb{R}^\infty} \tag{28}$$

for $\|\boldsymbol{x}\|\leq\beta_1$.

Author's personal copy

According to the exponential stability property of the $\boldsymbol{x}_f$-subsystem (20), and the converse Lyapunov theorem [42], we have that there exist a Lyapunov function candidate $V_f(\boldsymbol{x}_f)$ and positive real numbers l_1, l_2, l_3 and l_4, such that the following conditions hold:

$$\begin{cases} l_1||\boldsymbol{x}_f||^2_{\mathbb{R}^\infty} \le V_f(\boldsymbol{x}_f) \le l_2||\boldsymbol{x}_f||^2_{\mathbb{R}^\infty} \\ \dot{V}_f(\boldsymbol{x}_f) = \dfrac{1}{\varepsilon}\nabla V_f^T \boldsymbol{A}_{f\varepsilon}\boldsymbol{x}_f \le -\dfrac{l_3}{\varepsilon}||\boldsymbol{x}_f||^2_{\mathbb{R}^\infty} \\ ||\nabla V_f||_{\mathbb{R}^\infty} \le l_4||\boldsymbol{x}_f||_{\mathbb{R}^\infty} \end{cases} \tag{29}$$

where $\nabla V_f \triangleq \partial V_f/\partial x_f$.

It follows from the fact $\bar{\boldsymbol{B}}_2(z) = \boldsymbol{\Phi}_s^T(z)\boldsymbol{B}_2 + \boldsymbol{\Phi}_f^T(z)\boldsymbol{B}_{2f}$ that

$$\int_{\underline{z}}^{\bar{z}} \bar{\boldsymbol{B}}_2^T(z)\bar{\boldsymbol{B}}_2(z)dz = \boldsymbol{B}_2^T\boldsymbol{B}_2 + \boldsymbol{B}_{2f}^T\boldsymbol{B}_{2f}$$

Thus, we have

$$\left\|\boldsymbol{B}_{2f}^T\nabla V_f\right\| = \left((\nabla V_f)^T\boldsymbol{B}_{2f}\boldsymbol{B}_{2f}^T\nabla V_f\right)^{\frac{1}{2}} \le l_5\left\|\nabla V_f\right\|_{\mathbb{R}^\infty} \le l_4 l_5\left\|\boldsymbol{x}_f\right\|_{\mathbb{R}^\infty} \tag{30}$$

where $l_5 \triangleq \left(\bar{\lambda}\left(\int_{\underline{z}}^{\bar{z}}\bar{\boldsymbol{B}}_2^T(z)\bar{\boldsymbol{B}}_2(z)dz - \boldsymbol{B}_2^T\boldsymbol{B}_2\right)\right)^{1/2}$

Now, choose the smooth function $V(\boldsymbol{x}, \boldsymbol{x}_f) \triangleq V^*(\boldsymbol{x}) + V_f(\boldsymbol{x}_f)$ as the Lyapunov function candidate of the system (27), where $V^*(\boldsymbol{x})$ is the solution of the HJI equation (24). Differentiating $V(\boldsymbol{x}_s, \boldsymbol{x}_f)$ with respect to time along the trajectories of system (27) yields, $\dot{V}(\boldsymbol{x}, \boldsymbol{x}_f) = \dot{V}^*(\boldsymbol{x}) + \dot{V}_f(\boldsymbol{x}_f)$

$$\begin{aligned} &= (\nabla V^*)^T\dot{\boldsymbol{x}} + (\nabla V_f)^T\dot{\boldsymbol{x}}_f \\ &= (\nabla V^*)^T(\boldsymbol{f}_s(\boldsymbol{x}, 0) + \boldsymbol{B}_2\boldsymbol{u}^* + (\boldsymbol{f}_s(\boldsymbol{x}, \boldsymbol{x}_f) - \boldsymbol{f}_s(\boldsymbol{x}, 0))) \\ &\quad + (\nabla V_f)^T\left(\frac{1}{\varepsilon}\boldsymbol{A}_{f\varepsilon}\boldsymbol{x}_f + \boldsymbol{f}_f(\boldsymbol{x}, \boldsymbol{x}_f) + \boldsymbol{B}_{2f}\boldsymbol{u}^*\right) \end{aligned} \tag{31}$$

Before deriving the condition for $\dot{V}(\boldsymbol{x}, \boldsymbol{x}_f) < 0$, we compute each part of (31) as follows. According to the HJI equation (24) and control law (25), we have

$$\begin{aligned} &(\nabla V^*)^T(\boldsymbol{f}_s(\boldsymbol{x}, 0) + \boldsymbol{B}_2\boldsymbol{u}^*) = (\nabla V^*)^T\boldsymbol{f}_s(\boldsymbol{x}, 0) - \frac{1}{2}(\nabla V^*)^T\boldsymbol{B}_2\boldsymbol{R}^{-1}\boldsymbol{B}_2^T\nabla V^*(\boldsymbol{x}) = -\boldsymbol{x}^T\boldsymbol{Q}_s\boldsymbol{x} - \frac{1}{4}(\nabla V^*)^T\boldsymbol{B}_2\boldsymbol{R}^{-1}\boldsymbol{B}_2^T\nabla V^* - \frac{1}{4\gamma_s^2}(\nabla V^*)^T\boldsymbol{B}_1\boldsymbol{B}_1^T\nabla V^* \\ &\le -\upsilon_1||\boldsymbol{x}||^2 - \left(\frac{1}{4}\upsilon_2 + \frac{1}{4\gamma_s^2}\upsilon_3\right)||\nabla V^*||^2 \end{aligned} \tag{32}$$

where $\upsilon_1 \triangleq \underline{\sigma}(\boldsymbol{Q}_s)$, $\upsilon_2 \triangleq \underline{\sigma}(\boldsymbol{B}_2\boldsymbol{R}^{-1}\boldsymbol{B}_2^T)$ and $\upsilon_3 \triangleq \underline{\sigma}(\boldsymbol{B}_1\boldsymbol{B}_1^T)$. By (28), it is clear that

$$(\nabla V^*)^T(\boldsymbol{f}_s(\boldsymbol{x}, \boldsymbol{x}_f) - \boldsymbol{f}_s(\boldsymbol{x}, 0)) \le k_3\left\|\boldsymbol{x}_f\right\|_{\mathbb{R}^\infty}\left\|\nabla V^*\right\| \tag{33}$$

Using (18), (25), (29) and (30), we obtain

$$\begin{aligned} &(\nabla V_f)^T\left(\frac{1}{\varepsilon}\boldsymbol{A}_{f\varepsilon}\boldsymbol{x}_f + \boldsymbol{f}_f(\boldsymbol{x}, \boldsymbol{x}_f) + \boldsymbol{B}_{2f}\boldsymbol{u}^*\right) \\ &= \frac{1}{\varepsilon}(\nabla V_f)^T\boldsymbol{A}_{f\varepsilon}\boldsymbol{x}_f + (\nabla V_f)^T\boldsymbol{f}_f(\boldsymbol{x}, \boldsymbol{x}_f) - \frac{1}{2}(\nabla V_f)^T\boldsymbol{B}_{2f}\boldsymbol{R}^{-1}\boldsymbol{B}_2^T\nabla V^*(\boldsymbol{x}) \\ &\le -\frac{l_3}{\varepsilon}||\boldsymbol{x}_f||^2_{\mathbb{R}^\infty} + (k_1||\boldsymbol{x}|| + k_2||\boldsymbol{x}_f||_{\mathbb{R}^\infty})||\nabla V_f||_{\mathbb{R}^\infty} + \frac{1}{2}\upsilon_4||(\nabla V_f)^T\boldsymbol{B}_{2f}||||\nabla V^*|| \\ &\le \left(k_2 l_4 - \frac{l_3}{\varepsilon}\right)||\boldsymbol{x}_f||^2_{\mathbb{R}^\infty} + k_1 l_4||\boldsymbol{x}||||\boldsymbol{x}_f||_{\mathbb{R}^\infty} + \frac{1}{2}\upsilon_4 l_4 l_5||\boldsymbol{x}_f||_{\mathbb{R}^\infty}\left\|\nabla V^*\right\| \end{aligned} \tag{34}$$

where $\upsilon_4 \triangleq \bar{\sigma}(\boldsymbol{R}^{-1}\boldsymbol{B}_2^T)$

From (31)–(34), we have

$$\dot{V}(\boldsymbol{x}, \boldsymbol{x}_f) \le -\upsilon_1||\boldsymbol{x}||^2 + \left(k_2 l_4 - \frac{l_3}{\varepsilon}\right)||\boldsymbol{x}_f||^2 - \left(\frac{1}{4}\upsilon_2 + \frac{1}{4\gamma_s^2}\upsilon_3\right)||\nabla V^*||^2 + k_1 l_4||\boldsymbol{x}||||\boldsymbol{x}_f||_{\mathbb{R}^\infty} + \left(k_3 + \frac{1}{2}\upsilon_4 l_4 l_5\right)||\boldsymbol{x}_f||_{\mathbb{R}^\infty}||\nabla V^*|| = -\boldsymbol{\xi}^T\boldsymbol{\Sigma}(\varepsilon)\boldsymbol{\xi}$$

Author's personal copy

where $\boldsymbol{\xi} \triangleq \begin{bmatrix} ||\boldsymbol{x}|| \\ ||\boldsymbol{x}_f||_{\mathbb{R}^\infty} \\ ||\nabla V^*|| \end{bmatrix}$ and $\boldsymbol{\Sigma}(\varepsilon) \triangleq \begin{bmatrix} \upsilon_1 & -\frac{1}{2}k_1 l_4 & 0 \\ -\frac{1}{2}k_1 l_4 & \frac{l_3}{\varepsilon} - k_2 l_4 & -\frac{1}{2}k_3 - \frac{1}{4}\upsilon_4 l_4 l_5 \\ 0 & -\frac{1}{2}k_3 - \frac{1}{4}\upsilon_4 l_4 l_5 & \frac{1}{4}\upsilon_2 + \frac{1}{4\gamma_s^2}\upsilon_3 \end{bmatrix}$ Defining

$$\varepsilon_1 \triangleq \frac{4l_3\upsilon_1}{k_1^2 l_4^2 + 4k_2 l_4 \upsilon_1}$$

$$\varepsilon_2 \triangleq \frac{4\gamma_s^2 l_3 \upsilon_1 \upsilon_2 + 4 l_3 \upsilon_1 \upsilon_3}{4\gamma_s^2 k_3^2 \upsilon_1 + \gamma_s^2 l_4^2 l_5^2 \upsilon_1 \upsilon_4^2 + 4\gamma_s^2 k_3 l_4 l_5 \upsilon_1 \upsilon_4 + \gamma_s^2 k_1^2 l_4^2 \upsilon_2 + k_1^2 l_4^2 \upsilon_3 + 4\gamma_s^2 k_2 l_4 \upsilon_1 \upsilon_2 + 4k_2 l_4 \upsilon_1 \upsilon_3}$$

and $\varepsilon^* \triangleq \min\{\varepsilon_1, \varepsilon_2\}$, we have that, if $\varepsilon \in (0, \varepsilon^*)$, then $\dot{V}(\boldsymbol{x}, \boldsymbol{x}_f) < 0$. This means that the system (27) is locally asymptotically stable, i.e., $\lim_{t\to\infty} ||\boldsymbol{x}(t)|| \to 0$ and $\lim_{t\to\infty} ||\boldsymbol{x}_f(t)||_{\mathbb{R}^\infty} \to 0$. Considering $||\boldsymbol{y}(\cdot, t)||_2^2 = ||\boldsymbol{x}(t)||^2 + ||\boldsymbol{x}_f(t)||_{\mathbb{R}^\infty}^2$, then we have that $\lim_{t\to\infty} ||\boldsymbol{y}(\cdot, t)||_2 \to 0$. This means that the disturbance-free closed-loop PDE system (1)–(3) with control law (25) is locally asymptotically stable in $\mathbb{L}_2$-norm. ■

4.2. Combining the SPUA and MWR for solving the HJI equation

For notation simplicity, define $\boldsymbol{f}(\boldsymbol{x}) \triangleq \boldsymbol{f}_s(\boldsymbol{x}, 0)$ in the rest of the paper. It is noted from Lemma 1 and Theorem 1 that the H_∞ control law (25) hinges on the solution of the HJI equation (24) for the value function $V^*(\boldsymbol{x})$. In [20], Luo and Wu proposed an efficient SPUA, where the HJI equation was successively approximated by a sequence of linear PDEs. The procedure of the SPUA is given as follows:

Algorithm 1.

Step 1: Give an initial function $V^{(0)} \in \mathbb{V}_0$ ($\mathbb{V}_0 \subset \mathbb{V}$ is determined by Lemma 5 in [20]), and let $i = 0$.

Step 2: Update the control and disturbance policies with

$$\boldsymbol{u}^{(i)} = -\frac{1}{2}\boldsymbol{R}^{-1}\boldsymbol{B}_2^T \nabla V^{(i)} \tag{35}$$

$$\boldsymbol{w}^{(i)} = \frac{1}{2}\gamma_s^{-2}\boldsymbol{B}_1^T \nabla V^{(i)} \tag{36}$$

Step 3: Solve the following linear PDE for the cost function $V^{(i+1)}$:

$$(\nabla V^{(i+1)})^T(\boldsymbol{f} + \boldsymbol{B}_2\boldsymbol{u}^{(i)} + \boldsymbol{B}_1\boldsymbol{w}^{(i)}) + \boldsymbol{x}^T\boldsymbol{Q}_s\boldsymbol{x} + (\boldsymbol{u}^{(i)})^T\boldsymbol{R}\boldsymbol{u}^{(i)} - \gamma_s^2(\boldsymbol{w}^{(i)})^T\boldsymbol{w}^{(i)} = 0 \tag{37}$$

Step 4: Set $i = i + 1$, go back to Step 2 and continue.

Note that in Algorithm 1, we need to solve linear PDE (37) at each iterative step. Thus, we develop the MWR on a set Ω such that $x \in \Omega$. From the well known high-order Weierstrtrass approximation theorem [43], it follows that a continuous function can be uniformly approximated to any degree of accuracy by a set of linearly independent basis functions. We assume that there exists a complete set of linearly independent basis functions $\boldsymbol{\psi}(x) = \left\{\psi_k(x)\right\}_{k=1}^{\infty}$ such that $\psi_k(0) = 0$, $\forall k$. Then the solution of Eq. (37) can be expressed as a linear combination of basis functions $\boldsymbol{\psi}(x)$, i.e.,

$$V^{(i+1)}(\boldsymbol{x}) = \sum_{l=1}^{\infty} c_l^{(i+1)}\psi_l(\boldsymbol{x}) \tag{38}$$

where the sum is assumed to converge pointwise on the set Ω. A trial solution can be taken by truncating the series to

$$\hat{V}^{(i+1)}(\boldsymbol{x}) \triangleq \sum_{l=1}^{L} c_l^{(i+1)}\psi_l(\boldsymbol{x}) = (\boldsymbol{c}^{(i+1)})^T\boldsymbol{\psi}_L(\boldsymbol{x}) = \boldsymbol{\psi}_L^T(\boldsymbol{x})\boldsymbol{c}^{(i+1)} \tag{39}$$

where $\boldsymbol{c}^{(i+1)} = [c_1^{(i+1)} \cdots c_L^{(i+1)}]^T$ and $\boldsymbol{\psi}_L(\boldsymbol{x}) = [\psi_1(\boldsymbol{x}) \cdots \psi_L(\boldsymbol{x})]^T$. The partial derivative of $\hat{V}^{(i+1)}(\boldsymbol{x})$ is given by

$$\nabla\hat{V}^{(i+1)}(\boldsymbol{x}) = \sum_{l=1}^{L} c_l^{(i+1)}\nabla\psi_l(\boldsymbol{x}) = \nabla\boldsymbol{\psi}_L^T(\boldsymbol{x})\boldsymbol{c}^{(i+1)} \tag{40}$$

where $\nabla\boldsymbol{\psi}_L(\boldsymbol{x}) \triangleq [\nabla\psi_1(\boldsymbol{x}) \cdots \nabla\psi_L(\boldsymbol{x})]^T$ is the Jacobian of $\boldsymbol{\psi}_L$. Then according to (35) and (36) in Algorithm 1, the updates of disturbance and control policies are respectively given as

$$\hat{\boldsymbol{w}}^{(i)} = \frac{1}{2}\gamma_s^{-2}\boldsymbol{B}_1^T\nabla\boldsymbol{\psi}_L^T(\boldsymbol{x})\boldsymbol{c}^{(i)} \tag{41}$$

$$\hat{\boldsymbol{u}}^{(i)} = -\frac{1}{2}\boldsymbol{R}^{-1}\boldsymbol{B}_2^T\nabla\boldsymbol{\psi}_L^T(\boldsymbol{x})\boldsymbol{c}^{(i)} \tag{42}$$

Substituting Eqs. (40)–(42) into Eq. (37) results in the following residual error

$$\delta(\boldsymbol{x}) \triangleq (\nabla\hat{V}^{(i+1)})^T(\boldsymbol{f} + \boldsymbol{B}_2\hat{\boldsymbol{u}}^{(i)} + \boldsymbol{B}_1\hat{\boldsymbol{w}}^{(i)}) + \boldsymbol{x}^T\boldsymbol{Q}_s\boldsymbol{x} + (\hat{\boldsymbol{u}}^{(i)})^T\boldsymbol{R}\hat{\boldsymbol{u}}^{(i)} - \gamma_s^2(\hat{\boldsymbol{w}}^{(i)})^T\hat{\boldsymbol{w}}^{(i)} \tag{43}$$

Author's personal copy

If the trial function (39) is the exact solution, the above residual would be zero. In the MWR, the constant vector $c^{(i+1)}$ is computed in such a way that residual (43) is forced to be zero in some weighted average sense as follows:

$$\boldsymbol{e}(\boldsymbol{c}^{(i+1)}) \triangleq \langle \delta(\boldsymbol{x}), \boldsymbol{\omega}_L(\boldsymbol{x})\rangle_\Omega = 0 \tag{44}$$

where $\boldsymbol{\omega}_L(\boldsymbol{x}) = [\omega_1(\boldsymbol{x})\cdots\omega_L(\boldsymbol{x})]^T$ is called the weighted function vector. Substituting (43) into (44) gives

$$\begin{aligned}\boldsymbol{e}(\boldsymbol{c}^{(i+1)}) &= \langle(\nabla\hat{V}^{(i+1)})^T\boldsymbol{f}, \boldsymbol{\omega}_L\rangle_\Omega + \langle(\nabla\hat{V}^{(i+1)})^T\boldsymbol{B}_2\hat{\boldsymbol{u}}^{(i)}, \boldsymbol{\omega}_L\rangle_\Omega + \langle(\nabla\hat{V}^{(i+1)})^T\boldsymbol{B}_1\hat{\boldsymbol{w}}^{(i)}, \boldsymbol{\omega}_L\rangle_\Omega \\ &\quad + \langle\boldsymbol{x}^T\boldsymbol{Q}_s\boldsymbol{x}, \boldsymbol{\omega}_L\rangle_\Omega + \langle(\hat{\boldsymbol{u}}^{(i)})^T\boldsymbol{R}\hat{\boldsymbol{u}}^{(i)}, \boldsymbol{\omega}_L\rangle_\Omega - \gamma_s^2\langle(\hat{\boldsymbol{w}}^{(i)})^T\hat{\boldsymbol{w}}^{(i)}, \boldsymbol{\omega}_L\rangle_\Omega\end{aligned} \tag{45}$$

By using (40)–(42), each term of (45) can be given as

$$\langle(\nabla\hat{V}^{(i+1)})^T\boldsymbol{f}, \boldsymbol{\omega}_L\rangle_\Omega = \int_\Omega \boldsymbol{\omega}_L(\boldsymbol{x})\boldsymbol{f}^T(\boldsymbol{x})\nabla\hat{V}^{(i+1)}(\boldsymbol{x})d\boldsymbol{x} = \left(\int_\Omega \boldsymbol{\omega}_L(\boldsymbol{x})\boldsymbol{f}^T(\boldsymbol{x})\nabla\Psi_L^T(\boldsymbol{x})d\boldsymbol{x}\right)\boldsymbol{c}^{(i+1)}$$

$$\begin{aligned}&\left\langle(\nabla\hat{V}^{(i+1)})^T\boldsymbol{B}_2\hat{\boldsymbol{u}}^{(i)}, \boldsymbol{\omega}_L\right\rangle_\Omega = -\frac{1}{2}\int_\Omega \boldsymbol{\omega}_L(\boldsymbol{x})(\hat{\boldsymbol{u}}^{(i)}(\boldsymbol{x}))^T\boldsymbol{B}_2^T\nabla\hat{V}^{(i+1)}(\boldsymbol{x})d\boldsymbol{x} \\ &= -\frac{1}{2}\left(\int_\Omega \boldsymbol{\omega}_L(\boldsymbol{x})\left(\left(\sum_{l=1}^L c_l^{(i)}\nabla\psi_l(\boldsymbol{x})\right)^T \boldsymbol{B}_2\boldsymbol{R}^{-1}\boldsymbol{B}_2^T\nabla\boldsymbol{\psi}_L^T(\boldsymbol{x})\right)d\boldsymbol{x}\right)\boldsymbol{c}^{(i+1)} \\ &= -\frac{1}{2}\left(\sum_{l=1}^L c_l^{(i)}\int_\Omega \boldsymbol{\omega}_L(\boldsymbol{x})\nabla\psi_l^T(\boldsymbol{x})\boldsymbol{B}_2\boldsymbol{R}^{-1}\boldsymbol{B}_2^T\nabla\boldsymbol{\psi}_L^T(\boldsymbol{x})d\boldsymbol{x}\right)\boldsymbol{c}^{(i+1)}\end{aligned}$$

$$\begin{aligned}&\left\langle(\nabla\hat{V}^{(i+1)})^T\boldsymbol{B}_1\hat{\boldsymbol{w}}^{(i)}, \boldsymbol{\omega}_L\right\rangle_\Omega = \frac{1}{2}\gamma_s^{-2}\int_\Omega \boldsymbol{\omega}_L(\boldsymbol{x})(\hat{\mathrm{w}}^{(i)}(\boldsymbol{x}))^T\boldsymbol{B}_1^T\nabla\hat{V}^{(i+1)}(\boldsymbol{x})d\boldsymbol{x} \\ &= \frac{1}{2}\gamma_s^{-2}\left(\int_\Omega \boldsymbol{\omega}_L(\boldsymbol{x})\left(\left(\sum_{l=1}^L c_l^{(i)}\nabla\psi_l(\boldsymbol{x})\right)^T \boldsymbol{B}_1\boldsymbol{B}_1^T\nabla\boldsymbol{\psi}_L^T(\boldsymbol{x})\right)d\boldsymbol{x}\right)\boldsymbol{c}^{(i+1)} \\ &= \frac{1}{2}\gamma_s^{-2}\left(\sum_{l=1}^L c_l^{(i)}\int_\Omega \boldsymbol{\omega}_L(\boldsymbol{x})\nabla\psi_l^T(\boldsymbol{x})\boldsymbol{B}_1\boldsymbol{B}_1^T\nabla\boldsymbol{\psi}_L^T(\boldsymbol{x})d\boldsymbol{x}\right)\boldsymbol{c}^{(i+1)} \\ &\left\langle\boldsymbol{x}^T\boldsymbol{Q}_s\boldsymbol{x}, \boldsymbol{\omega}_L\right\rangle_\Omega = \int_\Omega \boldsymbol{\omega}_L(\boldsymbol{x})(\boldsymbol{x}^T\boldsymbol{Q}_s\boldsymbol{x})d\boldsymbol{x} \\ &\left\langle(\hat{\boldsymbol{u}}^{(i)})^T\boldsymbol{R}\hat{\boldsymbol{u}}^{(i)}, \boldsymbol{\omega}_L\right\rangle_\Omega = \frac{1}{4}\left(\sum_{l=1}^L c_l^{(i)}\int_\Omega \boldsymbol{\omega}_L(\boldsymbol{x})\nabla\psi_l^T(\boldsymbol{x})\boldsymbol{B}_2\boldsymbol{R}^{-1}\boldsymbol{B}_2^T\nabla\boldsymbol{\psi}_L^T(\boldsymbol{x})d\boldsymbol{x}\right)\boldsymbol{c}^{(i)} \\ &\left\langle(\hat{\boldsymbol{w}}^{(i)})^T\hat{\boldsymbol{w}}^{(i)}, \boldsymbol{\omega}_L\right\rangle_\Omega = \frac{1}{4}\gamma_s^{-4}\left(\sum_{l=1}^L c_l^{(i)}\int_\Omega \boldsymbol{\omega}_L(\boldsymbol{x})\nabla\psi_l^T(\boldsymbol{x})\boldsymbol{B}_1\boldsymbol{B}_1^T\nabla\boldsymbol{\psi}_L^T(\boldsymbol{x})d\boldsymbol{x}\right)\boldsymbol{c}^{(i)}\end{aligned}$$

Define

$$\begin{aligned}\boldsymbol{Z}_f &\triangleq \int_\Omega \boldsymbol{\omega}_L(\boldsymbol{x})\boldsymbol{f}^T(\boldsymbol{x})\nabla\Psi_L^T(\boldsymbol{x})d\boldsymbol{x} \\ \boldsymbol{Z}_{\boldsymbol{B}_2}^l &\triangleq \int_\Omega \boldsymbol{\omega}_L(\boldsymbol{x})\nabla\psi_l^T(\boldsymbol{x})\boldsymbol{B}_2\boldsymbol{R}^{-1}\boldsymbol{B}_2^T\nabla\boldsymbol{\psi}_L^T(\boldsymbol{x})d\boldsymbol{x} \\ \boldsymbol{Z}_{\boldsymbol{B}_1}^l &\triangleq \int_\Omega \boldsymbol{\omega}_L(\boldsymbol{x})\nabla\psi_l^T(\boldsymbol{x})\boldsymbol{B}_1\boldsymbol{B}_1^T\nabla\boldsymbol{\psi}_L^T(\boldsymbol{x})d\boldsymbol{x} \\ \boldsymbol{Z}_{\boldsymbol{Q}_s} &\triangleq \int_\Omega \boldsymbol{\omega}_L(\boldsymbol{x})(\boldsymbol{x}^T\boldsymbol{Q}_s\boldsymbol{x})d\boldsymbol{x}\end{aligned}$$

Then, Eq. (44) can be rewritten as

$$\left(\boldsymbol{Z}_f - \frac{1}{2}\sum_{l=1}^L c_l^{(i)}\boldsymbol{Z}_{\boldsymbol{B}_2}^l + \frac{1}{2}\gamma_s^{-2}\sum_{l=1}^L c_l^{(i)}\boldsymbol{Z}_{\boldsymbol{B}_1}^l\right)\boldsymbol{c}^{(i+1)} + \boldsymbol{Z}_{\boldsymbol{Q}_c} + \frac{1}{4}\left(\sum_{l=1}^L c_l^{(i)}\boldsymbol{Z}_{\boldsymbol{B}_2}^l\right)\boldsymbol{c}^{(i)} - \frac{1}{4}\gamma_s^{-2}\left(\sum_{l=1}^L c_l^{(i)}\boldsymbol{Z}_{\boldsymbol{B}_1}^l\right)\boldsymbol{c}^{(i)} = 0 \tag{46}$$

Hence, the unknown coefficient vector $\boldsymbol{c}^{(i+1)}$ is computed with

$$\boldsymbol{c}^{(i+1)} = \left(\boldsymbol{Z}_f - \frac{1}{2}\sum_{l=1}^L c_l^{(i)}\boldsymbol{Z}_{\boldsymbol{B}_2}^l + \frac{1}{2}\gamma_s^{-2}\sum_{l=1}^L c_l^{(i)}\boldsymbol{Z}_{\boldsymbol{B}_1}^l\right)^{-1}\left(\boldsymbol{Z}_{\boldsymbol{Q}_s} + \frac{1}{4}\left(\sum_{l=1}^L c_l^{(i)}\boldsymbol{Z}_{\boldsymbol{B}_2}^l\right)\boldsymbol{c}^{(i)} - \frac{1}{4}\gamma_s^{-2}\left(\sum_{l=1}^L c_l^{(i)}\boldsymbol{Z}_{\boldsymbol{B}_1}^l\right)\boldsymbol{c}^{(i)}\right) \tag{47}$$

and then the solution of Eq. (37) is directly obtained via (39).

Author's personal copy

With the basis function vector $\boldsymbol{\psi}_L(\boldsymbol{x})$, the solution $V^*(x)$ of the HJI equation (24) can be represented as

$$V^*(\boldsymbol{x}) = (\boldsymbol{c}^*)^T \boldsymbol{\psi}_L(\boldsymbol{x}) + \sigma(\boldsymbol{x}) \tag{48}$$

where $\boldsymbol{c}^* = [c_1^* \cdots c_L^*]^T$ is the unknown ideal constant weight vector, and $\sigma(x)$ is the approximation error. Here, we assume that the size L of $\boldsymbol{\psi}_L$ is large enough such that $\sigma(x)$ can be ignored (i.e., $\sigma(x) \to 0$). Then, the H_∞ control law (25) is given as

$$\boldsymbol{u}^*(\boldsymbol{x}) = -\frac{1}{2}\boldsymbol{R}^{-1}\boldsymbol{B}_2^T \nabla \boldsymbol{\psi}_L^T(\boldsymbol{x})\boldsymbol{c}^* \tag{49}$$

Based on the developed MWR above, a specific implementation procedure of Algorithm 1 is formulated as follows:

Algorithm 2.

Step 1: Preparation: Select an independent basis function set $\boldsymbol{\psi}_L$, compute integrals $\boldsymbol{Z}_f, \boldsymbol{Z}_{\boldsymbol{Q}_s}, \boldsymbol{Z}_{\boldsymbol{B}_1}^l, \boldsymbol{Z}_{\boldsymbol{B}_2}^l$, and give constant $\xi > 0$.
Step 2: Give an initial coefficient vector $c^{(0)}$ such that $\hat{V}^{(0)}(\boldsymbol{x}) = \boldsymbol{\psi}_L^T(\boldsymbol{x})\boldsymbol{c}(0) \in V_0$, and let $i = 0$.
Step 3: Update $\hat{\boldsymbol{u}}^{(i)}$ and $\hat{\boldsymbol{w}}^{(i)}$ via (41) and (42).
Step 4: Compute coefficient vector $\boldsymbol{c}^{(i+1)}$ with (47).
Step 5: Set $i = i + 1$. If $||\boldsymbol{c}^{(i)} - \boldsymbol{c}^{(i-1)}|| \le \xi$, let $\boldsymbol{c}^* = \boldsymbol{c}^{(i)}$ and stop iteration, else, go back to Step 3 and continue. Then, the solution of the HJI equation (24) is obtained via $V^*(\boldsymbol{x}) = (\boldsymbol{c}^*)^T \boldsymbol{\psi}_L(\boldsymbol{x})$, and the H_∞ control policy is given with (49).

Remark 3. Note that the developed Algorithm 2 is to compute the parameter vector $\boldsymbol{c}^*$ through recurrent iteration (47), and ξ is a parameter for convergence accuracy. After parameter vector $\boldsymbol{c}^*$ is convergent, the H_∞ control policy (49) can be used for real control. That is to say, Algorithm 2 is an offline control design method.

Remark 4. It is noted that the developed HJI approach requires the availability of modes, which further depends on the accuracy of the slow subsystem (21). Thus, there are two ways to improve the efficiency of the HJI approach. The first is to increase the accuracy of the slow subsystem, such as, computing highly accurate EEFs from representative huge ensemble, or increasing the order of the slow subsystem (21). The second is to introduce an observer, which will require the solution of another HJI inequality (or equation) [15,16]. However, it is still theoretically unclear whether the developed SPUA method can solve the L_2 disturbance attenuation problem with an observer or not, and this issue is left for our future investigation.

5. Simulation studies

In this section, the simulation studies on a nonlinear diffusion-reaction process and a temperature cooling fin of high-speed aerospace vehicle are provided to demonstrate the effectiveness of the developed HJI approach.

5.1. Nonlinear diffusion-reaction process

Consider the following nonlinear diffusion-reaction process [1,35,43]:

$$\begin{cases} \dfrac{\partial y(z,t)}{\partial t} = \dfrac{\partial}{\partial z}\left(k(y)\dfrac{\partial y(z,t)}{\partial z}\right) + \beta_T(z)(e^{-\rho/(1+y)} - e^{-\rho}) + \beta_U(b_2(z)u(t) - y) + b_1(z)w(t) \\ y_h(t) = \displaystyle\int_0^\pi \sqrt{10}y(z,t)dz \end{cases} \tag{50}$$

subject to the Dirichlet boundary conditions

$$y(0,t) = y(\pi,t) = 0 \tag{51}$$

and the initial condition

$$y_0(z) = 0.3\sin(3z) \tag{52}$$

where y is the PDE state, $z \in [0, \pi]$, $k(y)$ is the diffusion coefficient that may be constant or dependent on the state, $\beta_T(z)$ is the heat of reaction which is spatially-varying, β_U is the heat transfer coefficient, ρ is activation energy, $b_1(z)$ and $b_2(z)$ are disturbance and actuator distribution function respectively. These parameters are given as follows:

$$k(y) = 0.5 + 0.7/(y+1),\ \beta_T(z) = 16(\cos(z)+1),\ \beta_U = 1,\ \rho = 1,$$

$$b_1(z) = [H(z-0.2\pi) - H(z-0.3\pi)] + [H(z-0.7\pi) - H(z-0.8\pi)],$$

where $H(\cdot)$ is the standard Heaviside function. For these values, the operating steady-state $y(z,t) = 0$ is an unstable one, and the system converges to a stable non-uniform steady state (as can be seen in Fig. 1). The weighting matrix R in (4) is given as $R = 0.5$. The parameter γ_s in (23) is given as $\gamma_s = 2$, then $\gamma > 2$ for the L_2-gain performance (4).
For convenience, we define the following ratio of disturbance attenuation as

$$r_d(t) \triangleq \left(\frac{\int_0^t \left(||y_h(\tau)||^2 + u^T(\tau)Ru(\tau)\right)d\tau}{\int_0^t ||w(\tau)||^2 d\tau}\right)^{1/2} \tag{53}$$

Author's personal copy

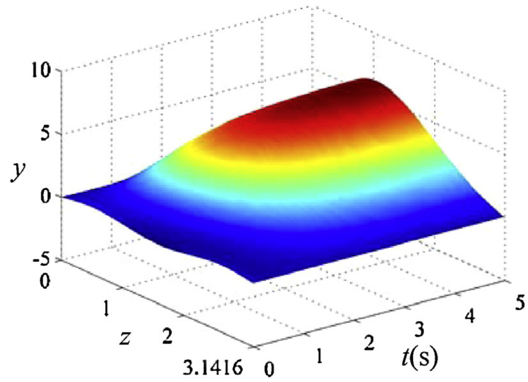

Fig. 1. State profile of open-loop PDE system.

which is used to show the relationship between L_2-gain and time. The disturbance signal $w(t)$ used in the simulation is shown in Fig. 2, which is generated with

$$w(t) = 3r_1(t)e^{-0.3t}\cos(r_2(t)t) \tag{54}$$

where $r_1(t)$ and $r_2(t)$ are time-varying random parameters in interval [0, 1].

By selecting different $b_2(z)$, we consider two cases of control method.

Case 1. distributed control with

$$b_2(z) = 12[H(z - 0.2\pi) - H(z - 0.3\pi)] + 12[H(z - 0.7\pi) - H(z - 0.8\pi)].$$

Case 2. point control with

$$b_2(z) = \delta(z - 0.3\pi) + \delta(z - 0.8\pi).$$

where $\delta(\cdot)$ is the standard Dirac Delta function.

To compute EEFs with KLD, an ensemble of size 2000 (i.e., $M = 2000$) is collected from 20 simulations with the following initial conditions, control inputs and disturbances:

$y_0(z) = 0.3r_1\sin(n_1 z)$, $u = 0.1r_2$ and $w(t) = 0.1r_3$

where $r_i, i = 1, 2, 3$ are random numbers in [0, 1], and $n_1 = 1, 2, 3$, which are different for each simulations. Fig. 3 shows the first two EEFs, where it is found that the first two EEFs account for more than 99.0% energy contained in the ensemble of snapshots (i.e., $\zeta = 0.01$ in (22)). Thus, the SDP (50)–(52) can be accurately represented by a 2-order model of ODE (i.e., $N = 2$). That is, the first two EEFs are employed to compute the state of the slow subsystem.

Remark 5. EEFs are representative patterns of the ensemble that collected from PDE system with different initial conditions, control inputs and disturbances. Thus, the ensemble is expected to contain representative snapshots that visit state space as much as possible. To this end, different random signals are applied in the simulations since they contain enough frequencies. In fact, any other sufficiently rich signals can also be used, such as the sum of sinusoidal signals with different frequencies. For specific PDE systems, two ways are possible to improve the quality of EEFs: increase the size of ensemble and enlarge the number of simulations with different sufficient rich signals.

Now, we use the developed HJI approach to solve the L_2 disturbance attenuation problem of Cases 1 and 2. Select the following basis function vector:

$$\boldsymbol{\psi}_8(\boldsymbol{x}) = [\,x_1^2 \quad x_1x_2 \quad x_2^2 \quad x_1^2x_2^2 \quad x_1x_2^3 \quad x_1^3x_2 \quad x_1^4 \quad x_2^4\,]^T \tag{55}$$

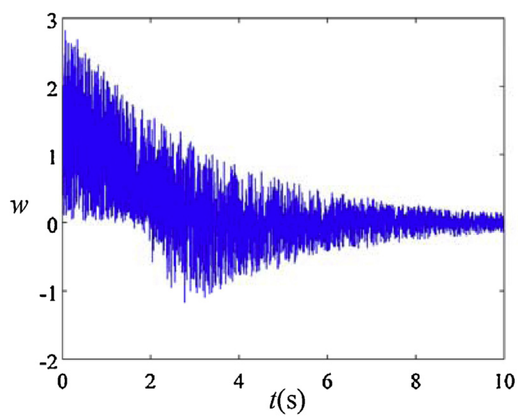

Fig. 2. Disturbance signal.

Author's personal copy

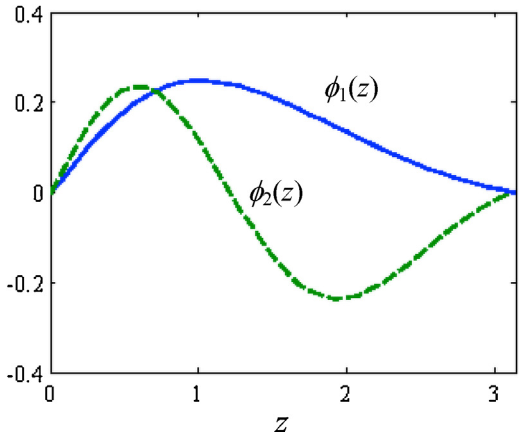

Fig. 3. The first two EEFs.

for approximating the value function of (39), the initial coefficient vector is chosen as

$$\boldsymbol{c}^{(0)} = [\,0.025 \quad 0 \quad 0 \quad 0 \quad 0 \quad 0 \quad 0 \quad 0\,]^T$$

for Case 1 and

$$\boldsymbol{c}^{(0)} = [\,0.55 \quad 0 \quad 0 \quad 0 \quad 0 \quad 0 \quad 0 \quad 0\,]^T$$

for Case 2. By applying the proposed Algorithm 2 to solve the HJI equation, we select the weighted function vector as $\boldsymbol{\omega}_8(\boldsymbol{x}) = \boldsymbol{\psi}_8(\boldsymbol{x})$ in the MWR. Fig. 4 gives the norm of coefficient vector (i.e., $||\boldsymbol{c}^{(i)}||$) at each iterative step. For Case 1, $c^{(i)}$ converges to

$$\boldsymbol{c}^* = \boldsymbol{c}^{(12)} = [\,0.2289 \quad -1.4646 \quad 8.5036 \quad 0.0367 \quad -0.2092 \quad -0.0155 \quad -0.0032 \quad 0.5990\,]^T$$

at the 12th iterative step (i.e., $i = 12$). For Case 2, $c^{(i)}$ converges to

$$\boldsymbol{c}^* = \boldsymbol{c}^{(7)} = [\,0.8120 \quad -0.7382 \quad 9.2050 \quad -0.0541 \quad 0.1548 \quad 0.0590 \quad 0.0109 \quad -0.4560\,]^T$$

at the 7th iterative step (i.e., $i = 11$).

With the vector $\boldsymbol{c}^*$, the control policy (denoted as u^*) is obtained via (49). Then, the closed-loop simulation is conducted under the disturbance signal of Fig. 2. The control actions u^*, the state trajectories of the slow subsystem, and the state profile of closed-loop PDE system are given in Figs. 5–7 respectively, from which it can be seen that all signals approach to the zero. Fig. 8 shows the curves of $r_d(t)$ for Cases 1 and 2. It is found that $r_d(t)$ converges to 1.1402 (<2) for Case 1 and to 1.2202 ($<$ 2) for Case 2 as time increases, which implies that the designed H_∞ control law can achieve an L_2-gain performance level γ larger than 2 for both Cases 1 and 2.

5.2. Temperature cooling fin of high-speed aerospace vehicle

In this subsection, the developed control method is applied to a complex temperature cooling fin of high-speed aerospace vehicle [32], the system dynamics of which is described with the following parabolic PDE:

$$\rho C \frac{\partial T(l,t)}{\partial t} = k\frac{\partial^2 T}{\partial l^2} - \frac{Ph}{A}(T - T_{\infty 1}) - \frac{P\varepsilon\sigma}{A}(T^4 - T_{\infty 2}^4) + \hat{b}_1(l)w(t) + \hat{\boldsymbol{B}}_2(l)\boldsymbol{u}(t) \tag{56}$$

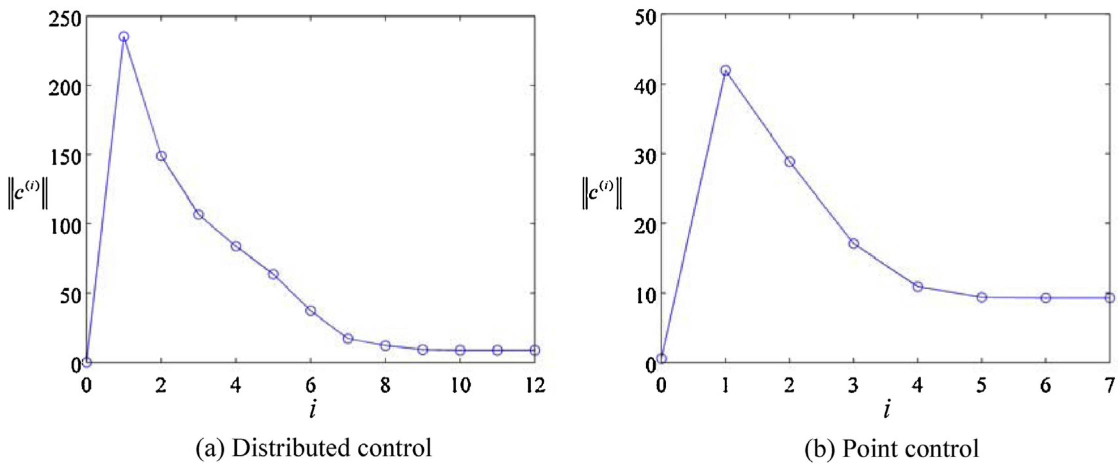

Fig. 4. The norm of coefficient vector $||c^{(i)}||$ at each iterative step.

Author's personal copy

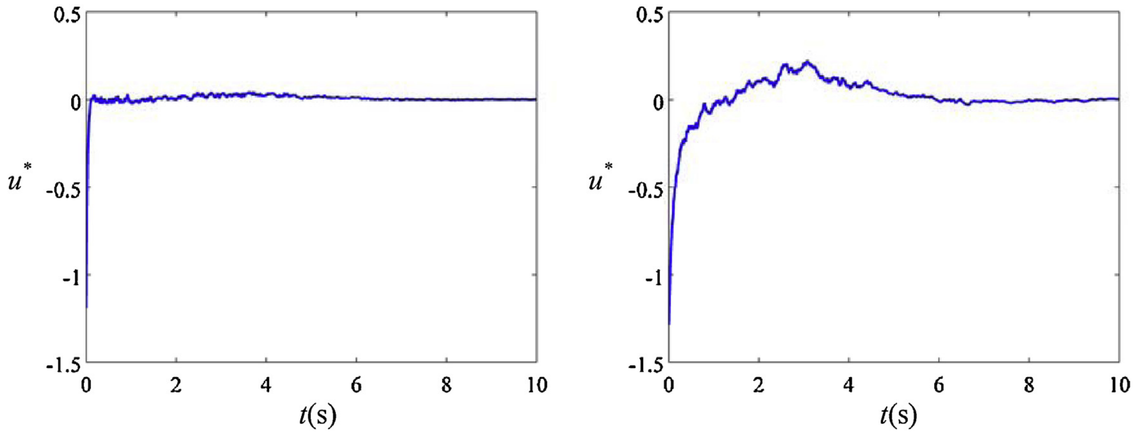

(a) Distributed control (b) Point control

Fig. 5. The actual control action u^*.

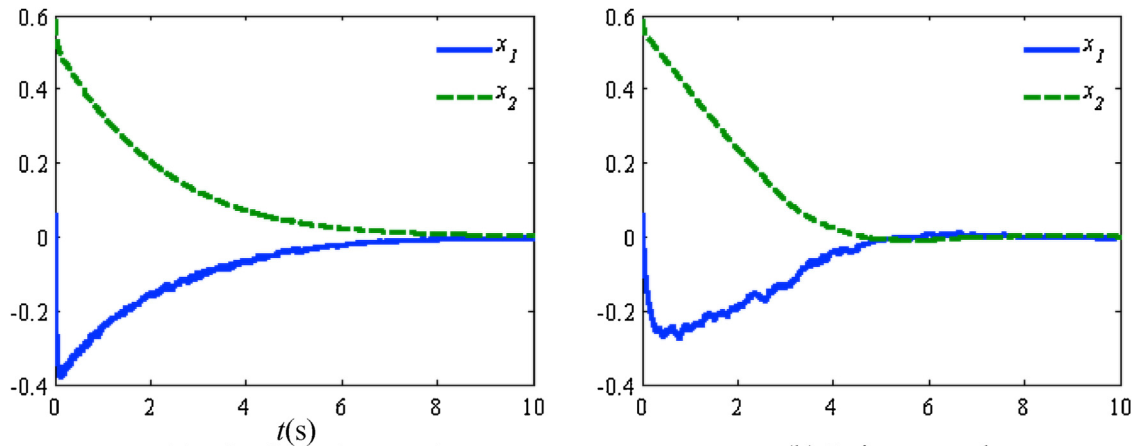

(a) Distributed control (b) Point control

Fig. 6. Actual state trajectories of closed-loop slow subsystem.

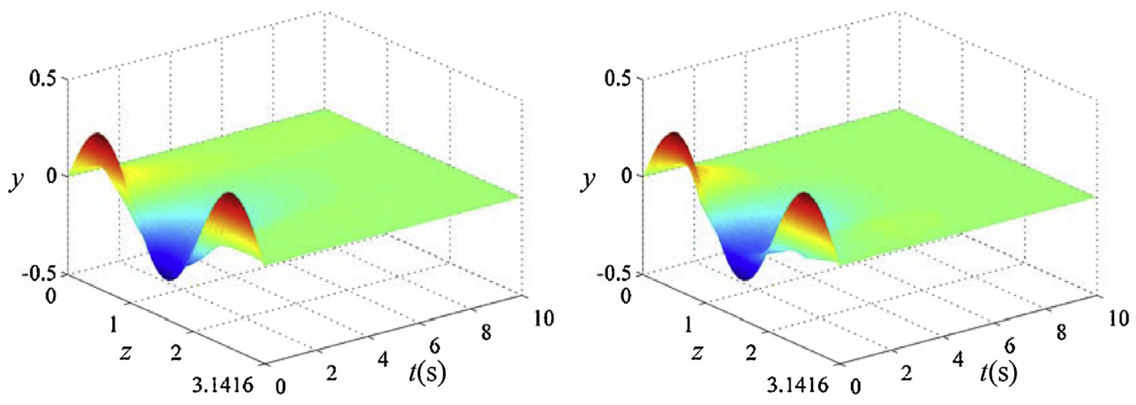

(a) Distributed control (b) Point control

Fig. 7. State profile of the closed-loop PDE system.

Author's personal copy

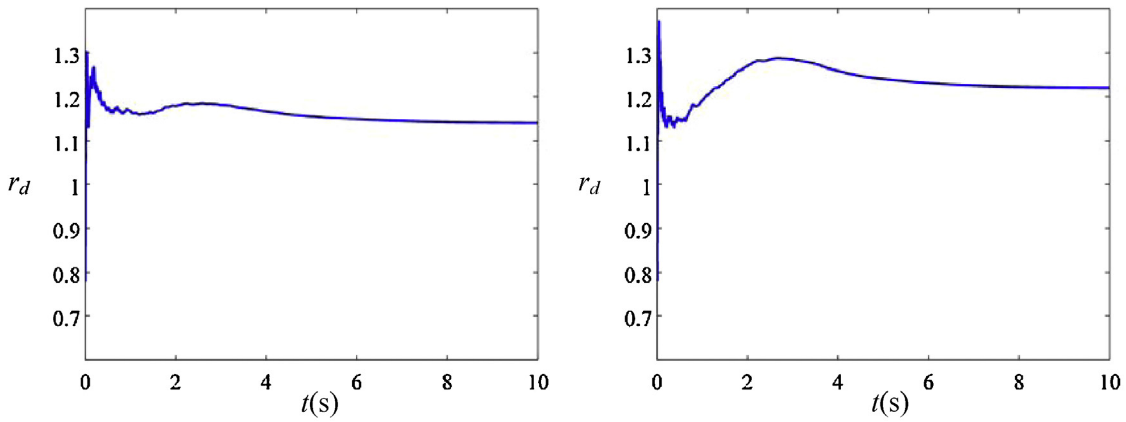

(a) Distributed control (b) Point control

Fig. 8. Curve of $r_d(t)$.

Table 1
System parameters and their values.

$k = 19\ \ \mathrm{W/(m^\circ C)}$	Thermal conductivity
$A = 1\ \ \mathrm{m^2}$	Cross sectional area
$P = 1.3716\ \ \mathrm{m}$	Perimeter
$L = 1\ \ \mathrm{m}$	Length
$h = 20\ \ \mathrm{W/(m^\circ C)}$	Convective heat transfer coefficient
$T_{\infty 1} = 100\ \ ^\circ\mathrm{C}$	Temperature of the medium in the immediate surrounding of the surface
$T_{\infty 2} = -40\ \ ^\circ\mathrm{C}$	Temperature at a far away place in the direction normal to the surface.
$\varepsilon = 0.965$	Emissivity of the material
$\sigma = 5.669 \times 10^{-8}\ \ \mathrm{W/m^2K^4}$	Boltzmann constant
$\rho = 7865\ \ \mathrm{kg/m^3}$	Density of the material
$C = 0.46\ \ \mathrm{kJ/(kg^\circ C)}$	Specific heat of the material

subject to the boundary conditions

$$\left.\frac{\partial T}{\partial l}\right|_{l=0} = 1, \quad \left.\frac{\partial T}{\partial l}\right|_{l=L} = 0 \tag{57}$$

and the initial condition

$$T(l, 0) = T_0(l). \tag{58}$$

where T is the temperature, $l \in [0, L]$, $\boldsymbol{u}(t) = [\, u_1(t) \quad u_2(t) \quad u_3(t)\,]^T$ is the control input vector, $w(t)$ is the exogenous disturbance, $\hat{b}_1(l)$ and $\hat{B}_2(l) = [\, \hat{b}_2^1(l) \quad \hat{b}_2^2(l) \quad \hat{b}_2^3(l)\,]^T$ describe how disturbance and control actions are distributed in spatial domain respectively. The control objective is to reach a constant desired temperature $T_d = 700\ \ ^\circ C$, and achieve L_2 disturbance attenuation. The system parameters and their values are given in Table 1.

It is worthwhile to define the dimensionless temperature, desired temperature and spatial position variables as:

$$\bar{y} = \frac{T}{\bar{T}}, \bar{y}_d = \frac{T_d}{\bar{T}} \quad \text{and} \quad z = \frac{l}{L}$$

where $\bar{T} = 1000$ can be a large number. Then, system (56)–(58) is rewritten as a dimensionless formulation:

$$\frac{\partial \bar{y}(z,t)}{\partial t} = \frac{k}{\rho C L^2}\frac{\partial^2 \bar{y}}{\partial z^2} - \frac{Ph}{\rho CA}\left(\bar{y} - \frac{T_{\infty 1}}{\bar{T}}\right) - \frac{P\varepsilon\sigma}{\rho CA\bar{T}}(\bar{T}^4\bar{y}^4 - T_{\infty 2}^4) + \frac{1}{\rho C\bar{T}}\hat{b}_1(Lz)w(t) + \frac{1}{\rho C\bar{T}}\hat{\boldsymbol{B}}_2(Lz)\boldsymbol{u}(t) \tag{59}$$

subject to the boundary conditions

$$\left.\frac{\partial \bar{y}}{\partial z}\right|_{z=0} = \frac{L}{\bar{T}}, \quad \left.\frac{\partial \bar{y}}{\partial z}\right|_{z=1} = 0 \tag{60}$$

and the initial condition

$$\bar{y}(z, t) = \bar{y}_0(z). \tag{61}$$

where $\bar{y}_0(z) = T_0(Lz)/\bar{T}$.

Define state error $y = \bar{y} - \bar{y}_d$, $\alpha_1 = \frac{k}{\rho C L^2}$, $\alpha_2 = -\frac{Ph}{\rho CA}$, $\alpha_3 = -\frac{P\varepsilon\sigma}{\rho CA\bar{T}}$ and $\alpha_4 = \frac{1}{\rho C\bar{T}}$.

Then, under the consideration of external disturbance, the system (59)–(61) is briefly represented as

Author's personal copy

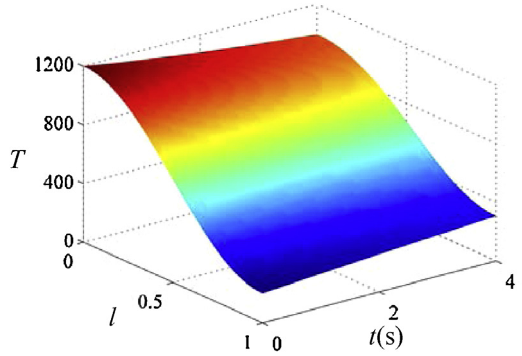

Fig. 9. Temperature profile of open-loop temperature cooling fin system.

$$\frac{\partial y(z,t)}{\partial t} = \alpha_1 \frac{\partial^2 y}{\partial z^2} + \alpha_2 y + \alpha_3 \bar{T}^4 (y+\bar{y}_d)^4 + u_d + \bar{b}_1(z) w(t) + \bar{\boldsymbol{B}}_2(z)\boldsymbol{u}(t) \tag{62}$$

subject to the boundary conditions

$$\left.\frac{\partial y}{\partial z}\right|_{z=0} = \frac{L}{\bar{T}}, \left.\frac{\partial y}{\partial z}\right|_{z=1} = 0 \tag{63}$$

and the initial condition

$$y(z,t) = y_0(z) \tag{64}$$

where $y_0(z) = \bar{y}_0(z) - y_d$, $w(z, t)$ is external disturbance, and $u_d = \alpha_2(\bar{y}_d - (T_{\infty 1}/\bar{T})) - \alpha_3 T^4_{\infty 2}$, $\bar{b}_1(z) = \alpha_4 \hat{b}_1(Lz)$, and $\bar{\boldsymbol{B}}_2(z) = \alpha_4 \hat{\boldsymbol{B}}_2(Lz)$.

For the L_2 disturbance attenuation problem of system (62)–(64), let R be an unit matrix, $\gamma_s = 10$ (i.e., $\gamma > 10$), and objective output $y_h(t) = \int_0^{\pi} y(z,t)dz$. Thus, the objective is to design control policy $\boldsymbol{u}$ such that $y(z, t)$ approaches zero and the L_2-gain is satisfied. $\bar{b}_1(z)$ and $\bar{B}_2(z)$ are given by $\bar{b}_1(z) = \cos(\pi z)$ and $\bar{\boldsymbol{B}}_2(z) = [\cos(\pi z) \quad \cos(1.5\pi z) \quad \cos(2\pi z)]^T$ respectively. With the initial state $y_0(z) = 0.5\cos(\pi z)$, i.e., $T_0(l) = 0.5\bar{T}\cos(\pi l/L) + T_d$, The state profile of open-loop PDE system is given in Fig. 9.

To compute EEFs with KLD, an ensemble of size 2000 (i.e., $M = 2000$) is collected from 20 simulations with the following initial conditions, control inputs and disturbances:

$y_0(z) = \cos(5r_1 z + r_2)$, $\boldsymbol{u} = [r_3 \quad r_4 \quad r_5]^T$ and $w(t) = r_6$

where r_i, $i = 1, \ldots, 6$ are random numbers in [0,1] which are different for each simulations. The first three EEFs are shown in Fig. 10, and it is found that the first three EEFs account for more than 99.0% energy contained in the ensemble of snapshots (i.e., $\zeta = 0.01$ in (22)). This means that the SDP (56)–(58) can be accurately represented by a 3-order model of ODE (i.e., N = 3). Thus, the first three EEFs are employed to compute the state of the slow subsystem.To design the H_∞ control policy with the HJI approach developed in Section 4, we select the following basis function vector:

$$\begin{aligned}\boldsymbol{\psi}_{18}(x) = [\, & x_1^2 \quad x_1x_2 \quad x_1x_3 \quad x_2^2 \quad x_2x_3 \quad x_3^2 \quad x_1^2x_2^2 \quad x_1^2x_3^2 \quad x_2^2x_3^2 \\ & x_1x_2^3 \quad x_1x_3^3 \quad x_2x_3^3 \quad x_1^3x_2 \quad x_1^3x_3 \quad x_2^3x_3 \quad x_1^4 \quad x_2^4 \quad x_3^4 \,]^T\end{aligned} \tag{65}$$

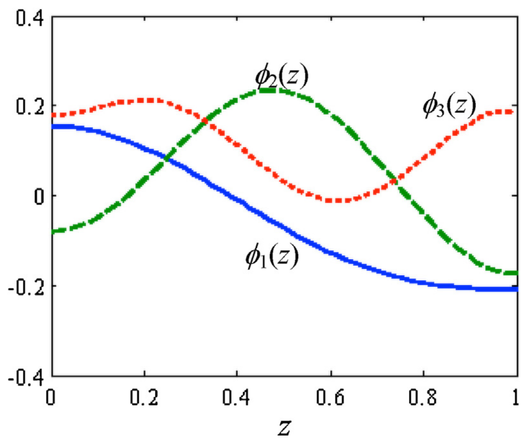

Fig. 10. The first three two EEFs of temperature cooling fin system.

Author's personal copy

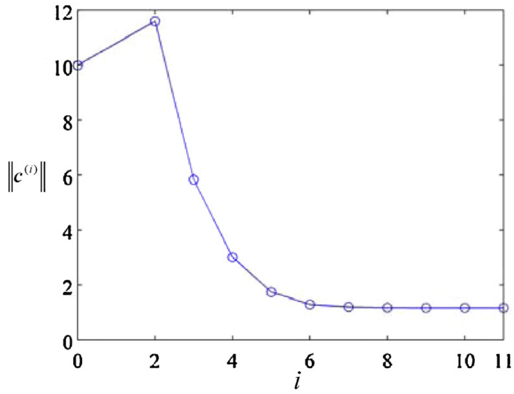

Fig. 11. The norm of coefficient vector $||\boldsymbol{c}^{(i)}||$ at each iterative step.

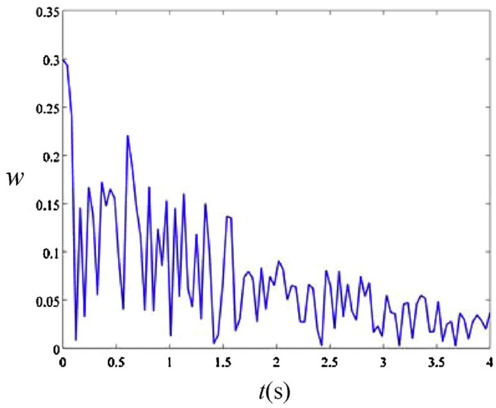

Fig. 12. Disturbance signal.

for approximating the value function of (39), and the elements of the initial coefficient vector are chosen as $c_1^{(0)} = 2$ and $c_j^{(0)} = 0, i = 2, \ldots, 18$. By applying the proposed Algorithm 2 to solve the HJI equation, the weighted function vector in MWR is chosen as $\boldsymbol{\omega}_{18}(x) = \boldsymbol{\psi}_{18}(x)$ of (65). Fig. 11 gives the norm of coefficient vector (i.e., $\left\|\boldsymbol{c}^{(i)}\right\|$) at each iterative step, where $\boldsymbol{c}^{(i)}$ converges quickly to

$$\boldsymbol{c}^* = \boldsymbol{c}^{(11)}$$
$$= [\ 0.2055\ \ -0.0944\ \ -0.4103\ \ 0.2652\ \ 0.5116\ \ 0.9059\ \ -0.0046\ \ -0.0152\ \ 0.0044\ \ -0.0014\ \ 0.0171\ \ -0.0109\ \ 0.0039\ \ 0.0139\ \ 0.0032\ \ 0.0001\ \ 0.0091\ \ -0.0211\ ]^T$$

at the 11th iterative step (i.e., $i = 11$). With the vector $\boldsymbol{c}^*$, the control policy (denoted as u^*) is obtained via (49). Then, the closed-loop simulation is conducted under the disturbance signal (as shown in Fig. 12) that generated by $w(t) = 0.3r_1(t)e^{-0.5t}$, where $r_1(t)$ is time-varying a random parameter in interval [0,1]. The control actions $\boldsymbol{u}^*$ and the state trajectories of the slow subsystem are given in Figs. 13 and 14 respectively, from which it can be seen that all signals approach to the zero. Fig. 15 shows the curve of $r_d(t)$, where it converges to 6.2467

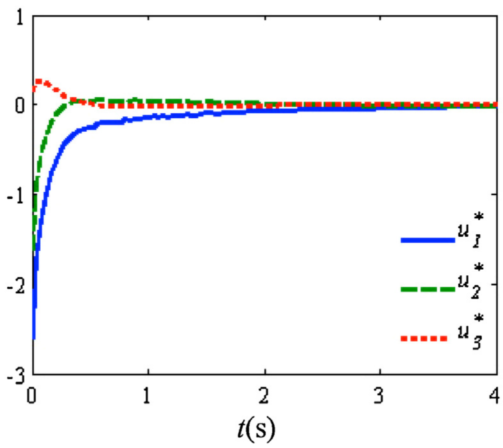

Fig. 13. The actual control actions u^*.

Author's personal copy

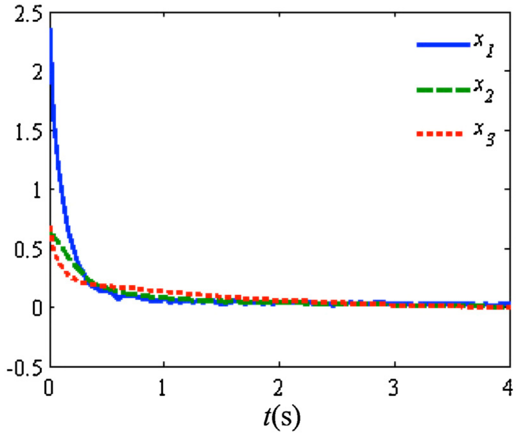

Fig. 14. Actual state trajectories of the closed-loop slow subsystem.

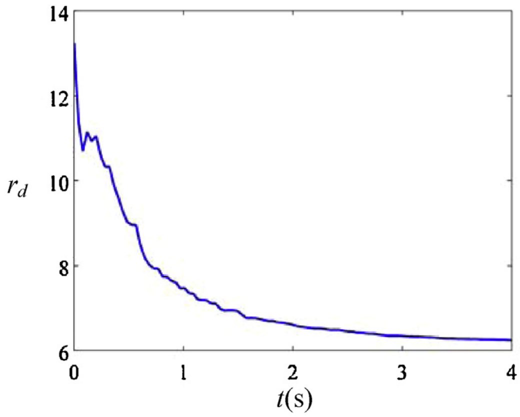

Fig. 15. Curve of $r_d(t)$.

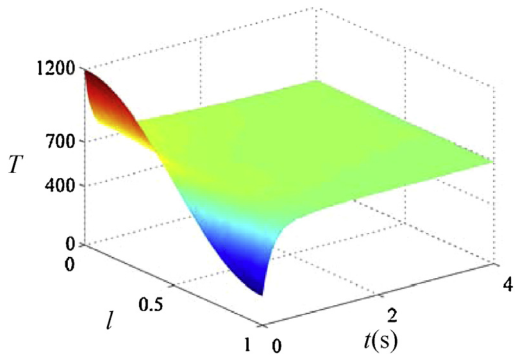

Fig. 16. Temperature profile of the closed-loop temperature cooling fin system.

(<10) as time increases, which implies that the designed H_∞ control law can achieve an L_2-gain performance level γ larger than 10 for the closed-loop system. The temperature profile of the closed-loop system is given Fig. 16, where the T converges to desired temperature $T_d = 700\ {}^\circ C$.

6. Conclusion

In this paper, the L_2 disturbance attenuation problem of a general class of highly dissipative nonlinear PDE systems has been addressed via the HJI approach. The KLD is firstly used to compute EEFs, based on which the slow subsystem is derived via the SP technique. Then, the HJI approach is proposed for synthesizing a finite-dimensional H_∞ controller based on the slow subsystem. The resulting H_∞ controller can not only guarantee the asymptotic stability of the original closed-loop PDE system, but also satisfy a prescribed level of disturbance attenuation. Subsequently, the SPUA and MWR are combined to solve the HJI equation. Finally, we apply the proposed H_∞ control method to a nonlinear diffusion-reaction process and a temperature cooling fin of high-speed aerospace vehicle, and the achieved results demonstrate its effectiveness.

Author's personal copy

Acknowledgment

This work was supported in part by the National Basic Research Program of China (973 Program) (2012CB720003), the National Natural Science Foundation of China under Grants (61121003; 91016004), the General Research Fund project from Science and Technology on Aircraft Control Laboratory of Beihang University under Grant 9140C480301130C48001, and Innovation Foundation of BUAA for Ph.D. Graduates under Grant YWF-13-RBYJ-009. The authors would like to thank anonymous reviewers for their valuable comments.

References

[1] A. Armaou, P.D. Christofides, Dynamic optimization of dissipative PDE systems using nonlinear order reduction, Chemical Engineering Science 57 (24) (2002) 5083–5114.
[2] P.D. Christofides, Nonlinear and Robust Control of PDE Systems: Methods and Applications to Transport-Reaction Processes, Birkhäuser, Boston, MA, 2001.
[3] A. Armaou, P.D. Christofides, Crystal temperature control in the Czochralski crystal growth process, Aiche Journal 47 (1) (2001) 79–106.
[4] W.H. Ray, Advanced Process Control, McGraw-Hill, New York, 1981.
[5] J. Baker, P.D. Christofides, Output feedback control of parabolic PDE systems with nonlinear spatial differential operators, Industrial & Engineering Chemistry Research 38 (11) (1999) 4372–4380.
[6] A. Kalani, P.D. Christofides, Simulation, estimation and control of size distribution in aerosol processes with simultaneous reaction, nucleation, condensation and coagulation, Computers & Chemical Engineering 26 (7–8) (2002) 1153–1169.
[7] Y. Ou, C. Xu, E. Schuster, T.C. Luce, J.R. Ferron, M.L. Walker, D.A. Humphreys, Optimal tracking control of current profile in Tokamaks, IEEE Transactions on Control Systems Technology 19 (2) (2011) 432–441.
[8] A.M. Bayen, R.L. Raffard, C.J. Tomlin, Adjoint-based control of a new Eulerian network model of air traffic flow, IEEE Transactions on Control Systems Technology 14 (5) (2006) 804–818.
[9] H.-N. Wu, B. Luo, Heuristic dynamic programming algorithm for optimal control design of linear continuous-time hyperbolic PDE systems, Industrial & Engineering Chemistry Research 51 (27) (2012) 9310–9319.
[10] B. Luo, H.-N. Wu, Online policy iteration algorithm for optimal control of linear hyperbolic PDE systems, Journal of Process Control 22 (7) (2012) 1161–1170.
[11] K. Zhou, J.C. Doyle, K. Glover, Robust and Optimal Control, Prentice Hall Upper Saddle River, NJ, 1996.
[12] A.J. Van Der Schaft, L_2-Gain and Passivity Techniques in Nonlinear Control, Springer-Verlag, Berlin, 1996.
[13] T. Başar, P. Bernhard, H^∞ Optimal Control and Related Minimax Design Problems: A Dynamic Game Approach, second ed., Birkhäuser, Boston, 1995.
[14] A.J. Van Der Schaft, L_2-gain analysis of nonlinear systems and nonlinear state-feedback H_∞ control, IEEE Transactions on Automatic Control 37 (6) (1992) 770–784.
[15] A. Isidori, W. Kang, H_∞ control via measurement feedback for general nonlinear systems, IEEE Transactions on Automatic Control 40 (3) (1995) 466–472.
[16] A. Isidori, A. Astolfi, Disturbance attenuation and H_∞ control via measurement feedback in nonlinear systems, IEEE Transactions on Automatic Control 37 (9) (1992) 1283–1293.
[17] G. Bianchini, R. Genesio, A. Parenti, A. Tesi, Global H_∞ controllers for a class of nonlinear systems, IEEE Transactions on Automatic Control 49 (2) (2004) 244–249.
[18] M. Abu-Khalaf, F.L. Lewis, J. Huang, Policy iterations and the Hamilton–Jacobi–Isaacs equation for H_∞ state feedback control with input saturation, IEEE Transactions on Automatic Control 51 (12) (2006) 1989–1995.
[19] R.W. Beard, T.W. Mclain, Successive, Galerkin approximation algorithms for nonlinear optimal and robust control, International Journal of Control 71 (5) (1998) 717–743.
[20] B. Luo, H.-N. Wu, Computationally efficient simultaneous policy update algorithm for nonlinear H_∞ state feedback control with Galerkin's method, International Journal of Robust and Nonlinear Control 23 (9) (2013) 717–743.
[21] G.N. Saridis, C.G. Lee, An approximation theory of optimal control for trainable manipulators, IEEE Transactions on Systems Man and Cybernetics Part B-Cybernetics 9 (3) (1979) 152–159.
[22] R. Beard, G.N. Saridis, J. Wen, Approximate solutions to the time-invariant Hamilton–Jacobi–Bellman equation, Journal of Optimization Theory and Applications 96 (3) (1998) 589–626.
[23] R. Beard, G.N. Saridis, J. Wen, Galerkin approximations of the generalized Hamilton–Jacobi–Bellman equation, Automatica 33 (12) (1997) 2159–2177.
[24] B. Van Keulen, H_∞-Control for Distributed Parameter Systems: A State Space Approach, Birkhauser, Boston, 1993.
[25] B.S. Chen, Y.T. Chang, Fuzzy state space modeling and robust observer-based control design for nonlinear partial differential systems, IEEE Transactions on Fuzzy Systems 17 (5) (2009) 1025–1043.
[26] H.-N. Wu, J.-W. Wang, H.-X. Li, Design of distributed H_∞ fuzzy controllers with constraint for nonlinear hyperbolic PDE systems, Automatica 48 (10) (2012) 2535–2543.
[27] H.-N. Wu, H.-X. Li, H_∞ fuzzy observer-based control for a class of nonlinear distributed parameter systems with control constraints, IEEE Transactions on Fuzzy Systems 16 (2) (2008) 502–516.
[28] Y.-T. Chang, B.-S. Chen, A fuzzy approach for robust reference-tracking-control design of nonlinear distributed parameter time-delayed systems and its application, IEEE Transactions on Fuzzy Systems 18 (6) (2010) 1041–1057.
[29] H.-N. Wu, H.-X. Li, Adaptive neural control design for nonlinear distributed parameter systems with persistent bounded disturbances, IEEE Transactions on Neural Networks 20 (10) (2009) 1630–1644.
[30] M. Li, P.D. Christofides, Optimal control of diffusion-convection-reaction processes using reduced-order models, Computers & Chemical Engineering 32 (9) (2008) 2123–2135.
[31] M. Li, P.D. Christofides, An input/output approach to the optimal transition control of a class of distributed chemical reactors, Chemical Engineering Science 62 (11) (2007) 2979–2988.
[32] V. Yadav, R. Padhi, S.N. Balakrishnan, Robust/optimal temperature profile control of a high-speed aerospace vehicle using neural networks, IEEE Transactions on Neural Networks 18 (4) (2007) 1115–1128.
[33] S. Pitchaiah, A. Armaou, Output feedback control of distributed parameter systems using adaptive proper orthogonal decomposition, Industrial & Engineering Chemistry Research 49 (21) (2010) 10496–10509.
[34] M. Krstic, On global stabilization of Burgers' equation by boundary control, Systems & Control Letters 37 (3) (1999) 123–141.
[35] P. Holmes, J.L. Lumley, G. Berkooz, Turbulence, Coherent Structures, Dynamical Systems and Symmetry, Cambridge University Press, Cambridge, UK, 1996.
[36] H.-X. Li, C.-K. Qi, Spatio-Temporal Modeling of Nonlinear Distributed Parameter Systems: A Time/Space Separation Based Approach, Springer Verlag, New York, 2011.
[37] A. Armaou, P.D. Christofides, Finite-dimensional control of nonlinear parabolic PDE systems with time-dependent spatial domains using empirical eigenfunctions, International Journal of Applied Mathematics and Computer Science 11 (2) (2001) 287–317.
[38] J. Baker, P.D. Christofides, Finite-dimensional approximation and control of non-linear parabolic PDE systems, International Journal of Control 73 (5) (2000) 439–456.
[39] B. Luo, H.N. Wu, Approximate optimal control design for nonlinear one-dimensional parabolic PDE systems using empirical eigenfunctions and neural network, IEEE Transactions on Systems Man and Cybernetics Part B-Cybernetics 42 (6) (2012) 1538–1549.
[40] J. Mercer, Functions of positive and negative type and their connection with the theory of integral equations, Philosophical Transactions of the Royal Society of London. Series A 209 (1909) 415–446.
[41] P.D. Christofides, Robust control of parabolic PDE systems, Chemical Engineering Science 53 (16) (1998) 2949–2965.
[42] H.K. Khalil, Nonlinear Systems, 3rd ed., Prentice-Hall, Upper Saddle River, NJ, 2002.
[43] R. Courant, D. Hilbert, Methods of Mathematical Physics, vol. 1, Wiley-VCH, Berlin, 1989.